

Synchronization Scheme based on Pilot Sharing in Cell-Free Massive MIMO Systems

Qihao Peng, Hong Ren, Zhendong Peng, Cunhua Pan, *Senior Member, IEEE*,
Maged El Kashlan, *Senior Member, IEEE*, Dongming Wang, *Senior Member, IEEE*, Jiangzhou Wang, *Fellow, IEEE*, and Xiaohu You, *Fellow, IEEE*.

Abstract

This paper analyzes the impact of pilot-sharing scheme on synchronization performance in a scenario where several slave access points (APs) with uncertain carrier frequency offsets (CFOs) and timing offsets (TOs) share a common pilot sequence. First, the Cramer-Rao lower bound (CRB) with pilot contamination is derived for pilot-pairing estimation. Furthermore, a maximum likelihood algorithm is presented to estimate the CFO and TO among the pairing APs. Then, to minimize the sum of CRBs, we devise a synchronization strategy based on a pilot-sharing scheme by jointly optimizing the cluster classification, synchronization overhead, and pilot-sharing scheme, while simultaneously considering the overhead and each AP's synchronization requirements. To solve this NP-hard problem, we simplify it into two sub-problems, namely cluster classification problem and the pilot sharing problem. To strike a balance between synchronization performance and overhead, we first classify the clusters by using the K-means algorithm, and propose a criteria to find a good set of master APs. Then, the pilot-sharing scheme is obtained by using the swap-matching operations. Simulation results validate the accuracy of our derivations and demonstrate the effectiveness of the proposed scheme over the benchmark schemes.

Index Terms

Cell-free massive MIMO, synchronization, pilot assignment, graph theory, coordinated integrated sensing and communications.

Q. Peng and M. El Kashlan are with the School of Electronic Engineering and Computer Science at Queen Mary University of London, U.K. (e-mail: {q.peng, maged.elkashlan}@qmul.ac.uk). Zhendong Peng is with the Department of Electrical and Computer Engineering, The University of British Columbia, Vancouver, BC V6T 1Z4, Canada (e-mail: zhendongpeng@ece.ubc.ca). Jiangzhou Wang is with the School of Engineering, University of Kent, CT2 7NT Canterbury, U.K. (e-mail: j.z.wang@kent.ac.uk). H. Ren, C. Pan, Dongming Wang, and Xiaohu You are with National Mobile Communications Research Laboratory, Southeast University, Nanjing, China. (e-mail: {hren,cpan,wangdm,xhyu}@seu.edu.cn). (Corresponding author: Hong Ren and Cunhua Pan)

I. INTRODUCTION

Recently, cell-free massive multiple-input multiple-output (mMIMO) systems have emerged as a promising technology for the sixth generation (6G) systems to simultaneously meet the ever-growing demand on data rate, latency, and decoding error probability [1]–[4]. By geographically deploying a multitude of distributed access points (APs) and eliminating the cell boundary, the distributed APs can seamlessly cooperate to mitigate inter-cell interference [5]–[7], and then jointly perform the coordinated multi-point transmission/reception (CoMP) by exploiting the multiple enhanced path gains, which consequently improves the spectral efficiency and user experience. However, as each AP is based on its own local oscillator (LO), the carrier frequency offset (CFO) and timing offset (TO) among distributed APs leads to asynchronous reception, which severely deteriorates the cooperative transmission and reception performance [8], [9]. Therefore, to reap the promising gains provided by CoMP, it is crucial to address the fundamental synchronization challenges in distributed architectures.

One method is to connect all distributed APs by physical wires, i.e., coaxial cables or optical fibers. Though this method seems logically straightforward, it has economic and technical challenges for practical implementation. Specifically, the deployment of extensive wired infrastructure incurs substantial costs in terms of installation and maintenance, especially in scenarios where APs are distributed over large geographical areas or in challenging terrains. Furthermore, the utilization of wired connections not only constrains the system's scalability and flexibility but also renders it highly vulnerable to environmental damage. Another solution is to deploy a global positioning system (GPS) disciplined oscillator at each AP as an accurate time source for individual devices [10], which is also typically expensive and impractical.

To address the above issues, extensive contributions have been devoted to the realization of wireless synchronization [11]–[19]. Generally, the widely used methods can be divided into two categories, namely reference signal-based synchronization [11]–[16] and pilot-based synchronization [17], [19]. Specifically, a master AP transmits an out-of-band reference signal, while slave APs can synchronize the frequency and phase by tracking the reference signal [11]. This approach still causes various errors due to different LOs. To mitigate the effect of LO, the authors of [12] proposed an AirShare scheme where the distributed receivers adjust LO to generate a frequency equal to the difference of two tones. Then, this strategy was further investigated in [13], [14] and also adopted in distributed microwave power transfer systems [15]. However, these

synchronization schemes based on reference signals utilize extra bandwidth and circuits, which causes lower spectral efficiency and higher power consumption. To tackle this issue, the authors of [17] proposed a pilot-pair synchronization strategy where the slave APs estimate the CFO and TO by receiving the burst pilot from the master APs. Then, the design of optimal pairs was studied in [18]. Inspired by the pilot-pair scheme, a similar strategy was applied to the distributed RadioWeaves infrastructure [19]. However, these synchronization schemes based on pairing pilot [17]–[19] did not analyze the impact of pilot allocation on the estimation performance.

Currently, various pilot allocation schemes have been adopted in cell-free mMIMO [20]–[25]. Particularly, it was demonstrated that pilot contamination is related to the distance among users that reuse the pilots [20]. Then, to minimize pilot contamination, the system performance can be maximized by using the Tabu-search-based algorithm [21] and the Hungarian algorithm [22]. Furthermore, to further reduce the pilot overhead, the pilot allocation relying on graphic theory was proposed in [23]. To meet the diverse requirements of users, pilot sharing schemes based on graphic theory were investigated in [24], [25]. Although pilot allocation schemes have been extensively studied in cell-free mMIMO systems and a similar pilot sharing scheme can be applied for pilot allocation, the relationship between synchronization performance and pilot allocation is still unknown. Furthermore, it is still challenging to design the optimal synchronization scheme with limited overhead.

To fill this gap, we first derive the Cramer-Rao bound (CRB) for the CFO and TO synchronization and then reveal the relationship between the estimation error and synchronous pilot allocation. Finally, a master-slave AP synchronization scheme based on a novel pilot-sharing strategy is proposed to enhance the synchronization performance with limited overhead. Our contributions are summarized as follows:

- 1) By considering the impact of pilot-sharing schemes on estimation errors, we analyze a more practical scenario where several slave APs with uncertain CFOs and TOs share a common pilot sequence. Then, a new CRB for pilot-pair estimation is derived while considering the pilot contamination. Finally, a maximum likelihood (ML) algorithm is provided to estimate the CFO and TO among two pairing APs.
- 2) As for the pilot-pairing synchronization scheme, our objective is to minimize the sum of CRBs by jointly optimizing clustering and the pilot allocation scheme while simultaneously considering all APs' synchronization requirements and limited overhead. To solve this NP-hard problem, we simplify it into two sub-problems, including the cluster classification

and the pilot sharing scheme. For the first sub-problem, the requirements on CFO and TO are transformed into the desired signal-to-interference -and-noise ratio (SINR), based on which we derive the maximum distance in the cluster. Then, the clusters are classified by iteratively performing the K-means algorithm, and a good set of master APs is found by using the proposed criteria. To solve the second sub-problem, a pilot sharing scheme based on the swap-matching operations is proposed to maximize the synchronization performance with limited overhead.

- 3) Our simulation results validate the accuracy of our derivations but also demonstrate that increasing the synchronous pilot length can decrease the estimation error. Furthermore, classifying clusters can shorten the distance between master APs and slave APs, which can enhance the path gain and significantly improve the estimation performance. Finally, our simulation results also confirm its superiority to other pilot-pair algorithms.

The remainder of this paper is organized as follows. In Section II, the system model is provided, and the CRB and ML estimations are given, respectively. By optimizing the cluster classification, pilot length and pilot sharing scheme, the sum of CRBs is minimized in Section III. Our simulation results are presented in Section IV. Finally, our conclusions are drawn in Section V.

II. SYSTEM MODEL

Since each AP has a unique oscillator and the synchronization is non-ideal, the very small residual CFO and TO will cause slow relative drift among different APs, which has a severe impact on cooperative transmissions. To prevent these errors from accumulating over time, the APs need to exchange the information and perform synchronization frequently. However, owing to the excessive number of APs, it is impractical for all APs to exchange the synchronization information with the central processing unit (CPU) directly by wireless channels, which leads to high overhead and low efficiency.

As illustrated in Fig. 1, to solve the scalability of cell-free mMIMO, K APs can be divided into K_C non-overlapping clusters, denoted as $\mathcal{C}_k, \forall k \in \{1, 2, \dots, K_C\}$, and $\mathcal{C}_k \cap \mathcal{C}_{k'} = \emptyset$, if $k \neq k'$. Furthermore, we assume that each cluster has only one master AP and several slave APs. We denote the master AP in the k -th cluster as j_k and the set of slave APs in the k -th cluster as \mathcal{S}_k with $\mathcal{S}_k \cup j_k = \mathcal{C}_k$ and $\mathcal{S}_k \cap j_k = \emptyset$. To synchronize all APs with low overhead, slave APs of \mathcal{S}_k first transmit the burst pilot to master APs, while the master APs estimate the CFO and

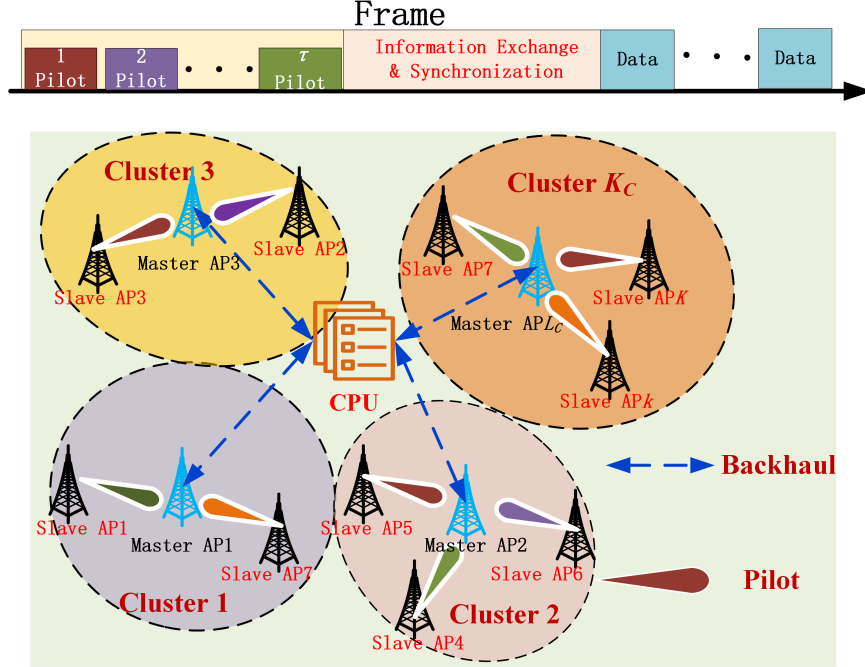


Fig. 1: Illustration of pilot-pair synchronization in cell-free mMIMO systems.

TO based on the received signals and then exchange information with the CPU. Then, the CPU performs the synchronization operation by transmitting the commands to the master APs.

We consider MIMO-OFDM APs, wherein the antennas at each AP operate according to a common LO. Owing to the slow relative drift among different APs and imperfect synchronization, we denote the CFO and TO between the i -th AP and the j_k -th AP as $\Delta f_{i,j_k}$ and $\Delta \tau_{i,j_k}$, respectively. Furthermore, since the antennas at each AP are based on a common local oscillator, the CFO and TO between the transmit antennas of the i -th AP and the j_k -th AP's receive antennas are the same. Therefore, for ease of derivation, we apply the received signal based on the single-antenna model for analysis.

We consider joint TO and CFO pilot-aided estimation for a transmitter-receiver pair, where the channel is multi-path time-invariant with additive white Gaussian noise (AWGN), with unknown path coefficients and multiple path delays. Generally, the number of the channel taps L_{i,j_k} between the i -th slave AP and the j_k -th master AP does not exceed the length of the cyclic prefix (CP). The multi-path channel impulse response from the i -th slave AP to the j_k -th master

AP can be represented by

$$h_{i,j_k}(t) = \sum_{l=0}^{L_{i,j_k}-1} \alpha_{i,j_k}^l \sqrt{\beta_{i,j_k}} \psi_{i,j_k}^l \delta(t - \varsigma_{i,j_k}^l), \quad (1)$$

where α_{i,j_k}^l and ς_{i,j_k}^l , $\forall l \in \{0, 1, 2, \dots, L_{i,j_k} - 1\}$, are the path gain coefficient and path delay of the l -th channel tap, respectively. β_{i,j_k} is the distance-dependent path loss, $\psi_{i,j_k}^l \in \mathcal{CN}(0, 1)$ denotes the small-scale fading factor, and $\delta(t)$ is the impulse response.

In the phase of network setup, the slave APs transmit the pilot sequence for synchronization based on a pilot burst transmission. Then, the j_k -th master AP receives time-domain baseband signal from several slave APs that share the common pilot sequence, which is given by

$$\begin{aligned} y_{j_k}(t) &= \sum_{i \in \mathcal{P}_p} h_{i,j_k}(t) \otimes s_p(t) e^{j2\pi \Delta f_{i,j_k} t} + w_{i,j_k}(t) \\ &= \sum_{i \in \mathcal{P}_p} \sum_{l=0}^{L_{i,j_k}-1} h_{i,j_k}^l s_p(t - \Delta \tau_{i,j_k} - \varsigma_{i,j_k}^l) e^{j2\pi \Delta f_{i,j_k} t} + w_{i,j_k}(t), \end{aligned} \quad (2)$$

where \mathcal{P}_p is the set of slave APs that share the p -th pilot sequence, $h_{i,j_k}^l = \alpha_{i,j_k}^l \sqrt{\beta_{i,j_k}} \psi_{i,j_k}^l$ is the l -th path coefficient, \otimes is the convolution operator, and $w_{i,j_k} \in \mathcal{CN}(0, \sigma^2)$ represents the additive noise. $s_p(t) = \frac{P_t}{\sqrt{T_s}} \sum_{n=0}^{N-1} s_p^n \prod\left(\frac{t}{T_s} - n\right)$ denotes the p -th pilot sequence, s_p^n is the time-domain chip symbol with $\mathbf{s}_p = \{s_p^0, s_p^1, \dots, s_p^{N-1}\}$, T_s is the chip interval, P_t is the transmission power, and N is the length of pilot sequence. $\prod(t)$ denotes the rectangular pulse, which can be expressed as

$$\prod(t) = \begin{cases} 1, & 0 \leq t \leq 1 \\ 0, & \text{otherwise.} \end{cases} \quad (3)$$

Then, the receiver performs chip-matched filtering, and sampling per one chip by substituting $t = mT_s$, $m \in \{0, \dots, M-1\}$. For ease of expression, we denote $\nabla(t) = \prod(t) \otimes \prod(t)$ as the convolution of two rectangular pulses. The received discrete-time signal is given by [17]

$$y_{j_k}[m] = \sum_{i \in \mathcal{P}_p} \left(\sum_{l=0}^{L_{i,j_k}-1} h_{i,j_k}^l \sum_{n=0}^{N-1} s_p^n \nabla\left(m - n - \frac{\Delta \tau_{i,j_k} + \varsigma_{i,j_k}^l}{T_s}\right) \right) e^{j2\pi \Delta f_{i,j_k} T_s m} + w_{i,j_k}[m]. \quad (4)$$

By using a coarse frame synchronization protocol, the receiver has a coarse knowledge of the frame timing such that it expects to find the pilot burst in a given interval including the guard time. The master AP collects M samples such that the sampled interval of duration MT_s

contains the pilot sequence.

Next, we collect the M received samples into an $M \times 1$ vector. The j_k -th master AP's received signal is defined as $\mathbf{y}_{j_k} = [y_{j_k}[0], y_{j_k}[1], \dots, y_{j_k}[M-1]]^T$. Then, the CFO matrix is defined as

$$\mathbf{F}(\Delta f_{i,j_k}) = \text{diag}(1, e^{j2\pi\Delta f_{i,j_k}T_s}, \dots, e^{j2\pi(M-1)\Delta f_{i,j_k}T_s}). \quad (5)$$

The $M \times (M - N + 1)$ matrix of the p -th pilot sequence is given by

$$\mathbf{S}_p = \begin{bmatrix} s_p^0 & 0 & \dots & 0 \\ s_p^1 & s_p^0 & & \vdots \\ \vdots & s_p^1 & & s_p^0 \\ s_p^{N-1} & \vdots & \dots & s_p^1 \\ 0 & s_p^{N-1} & & \vdots \\ \vdots & \vdots & & \\ 0 & 0 & \dots & s_p^{N-1} \end{bmatrix}. \quad (6)$$

The $[n, l]$ -th element of $(M - N + 1) \times L_{i,j_k}$ convolution matrix $\mathbf{U}(\Delta\tau_{i,j_k})$ is defined as

$$[\mathbf{U}(\Delta\tau_{i,j_k})]_{n,l} = \nabla \left(n - 1 - \frac{\Delta\tau_{i,j_k}}{T_s} - \frac{S_{i,j_k}^l}{T_s} \right). \quad (7)$$

Based on the above definitions, we arrive at the vector observation model as follows

$$\mathbf{y}_{j_k} = \sum_{i \in \mathcal{P}_p} \mathbf{F}(\Delta f_{i,j_k}) \mathbf{S}_p \mathbf{U}(\Delta\tau_{i,j_k}) \mathbf{h}_{i,j_k} + \mathbf{w}_{i,j_k}, \quad (8)$$

where $\mathbf{w}_{i,j_k} = [w_{i,j_k}[0], w_{i,j_k}[1], \dots, w_{i,j_k}[M-1]]^T$ is the vector of noise, and \mathbf{h}_{i,j_k} is a vector that collects the coefficients of L_{i,j_k} paths, denoted as $\mathbf{h}_{i,j_k} = [h_{i,j_k}^0, h_{i,j_k}^1, \dots, h_{i,j_k}^{L_{i,j_k}-1}]^T$. The derivations of (8) can be found in Appendix A.

III. CRAMER-RAO BOUND WITH PILOT CONTAMINATION

Based on the given model, we jointly estimate the synchronization parameters and derive the CRB for the CFO and TO. However, it is challenging to obtain CFO and TO from all slave APs, and thus the master APs can only estimate the synchronization parameters of the slave AP in the common cluster by treating the pilot contamination from other clusters as noise. The

received signal from the j_k -th master AP can be rewritten as

$$\mathbf{y}_{j_k} = \mathbf{F}(\Delta f_{i_{j_k}^p, j_k}) \mathbf{S}_p \mathbf{U}(\Delta \tau_{i_{j_k}^p, j_k}) \mathbf{h}_{i_{j_k}^p, j_k} + \underbrace{\sum_{i \in \{\mathcal{P}_p \setminus i_{j_k}^p\}} \mathbf{F}(\Delta f_{i, j_k}) \mathbf{S}_p \mathbf{U}(\Delta \tau_{i, j_k}) \mathbf{h}_{i, j_k}}_{\bar{\mathbf{w}}_{i, j_k}} + \mathbf{w}_{i, j_k}, \quad (9)$$

where $i_{j_k}^p$ is the slave AP using the p -th pilot sequence in cluster \mathcal{C}_k ¹.

A. Cramer-Rao Bound

In this subsection, we derive the CRB for the synchronization parameters with pilot contamination. However, owing to the unknown TO and CFO from the slave APs that share the common pilot sequence, it is challenging to derive the exact distribution. By assuming that the pilot contamination follows the complex Gaussian distribution², we adopt the well-known conclusion for the Fisher matrix of the Gaussian probability density function to derive CRB.

In our model, we denote $\Xi = \text{var}\{\bar{\mathbf{w}}_{i, j_k}\}$ as the variance of $\bar{\mathbf{w}}_{i, j_k}$ and define $\mathbf{m}(\boldsymbol{\theta}) = \mathbf{F}(\Delta f_{i_{j_k}^p, j_k}) \mathbf{S}_p \mathbf{U}(\Delta \tau_{i_{j_k}^p, j_k}) \mathbf{h}_{i_{j_k}^p, j_k}$, where the elements of $\boldsymbol{\theta}$ are given by

$$\theta_1 = \frac{\Delta \tau_{i_{j_k}^p, j_k}}{T_s}, \theta_2 = \Delta f_{i_{j_k}^p, j_k} T_s, \theta_{2l+3} = \text{Re}\{h_{i_{j_k}^p, j_k}^l\}, \theta_{2l+3} = \text{Im}\{h_{i_{j_k}^p, j_k}^l\}, \forall l \in \{0, \dots, L_{i_{j_k}^p, j_k} - 1\}. \quad (10)$$

Then, the $[n, m]$ -th element of the Fisher matrix can be expressed as

$$[\mathbf{J}]_{n, m}(\boldsymbol{\theta}) = 2\text{Re}\left\{\left(\frac{\partial \mathbf{m}(\boldsymbol{\theta})}{\partial \theta_n}\right)^H \Xi^{-1} \left(\frac{\partial \mathbf{m}(\boldsymbol{\theta})}{\partial \theta_m}\right)\right\}. \quad (11)$$

Based on the above discussion, we then derive the variance of pilot contamination by assuming that the TO and CFO follow the uniform distribution of $\frac{\Delta \tau_{i, j_k}}{T_s} \in [0, \eta]$, $\eta \in \mathbb{N}^+$,³ and $\Delta f_{i, j_k} \in [-f_{\max}, f_{\max}]$, $\forall i \in \{\mathcal{P}_p \setminus i_{j_k}^p\}$, respectively.

Obviously, the mean of $\bar{\mathbf{w}}_{i, j_k}$ is $\mathbf{0}$ as all variables are independent distribution with zero mean.

¹Similar to the frequency multiplexing, it is impossible to reuse the common pilot sequence in the same cluster, which is discussed in Section IV.

²Owing to no cell boundary and a large number of APs, a pilot sequence needs to be shared lots of times, and thus the pilot contamination can be approximated to follow a multivariate Gaussian distribution, by using the central limit theorem.

³Since the coarse synchronization is performed periodically by synchronization protocol, the residual TO drift within several chips.

The variance of $\mathbf{F}(\Delta f_{i,j_k}) \mathbf{S}_p \mathbf{U}(\Delta \tau_{i,j_k}) \mathbf{h}_{i,j_k}$, $\forall i \in \{\mathcal{P}_p \setminus i_{j_k}^p\}$, can be expressed as

$$\begin{aligned} & \text{var}\{\mathbf{F}(\Delta f_{i,j_k}) \mathbf{S}_p \mathbf{U}(\Delta \tau_{i,j_k}) \mathbf{h}_{i,j_k}\} \\ &= \mathbb{E}\{\mathbf{F}(\Delta f_{i,j_k}) \mathbf{S}_p \mathbf{U}(\Delta \tau_{i,j_k}) \mathbf{h}_{i,j_k} (\mathbf{F}(\Delta f_{i,j_k}) \mathbf{S}_p \mathbf{U}(\Delta \tau_{i,j_k}) \mathbf{h}_{i,j_k})^H\} \\ &= \mathbb{E}\{\mathbf{F}(\Delta f_{i,j_k}) \mathbf{S}_p \mathbf{U}(\Delta \tau_{i,j_k}) \mathbf{h}_{i,j_k} \mathbf{h}_{i,j_k}^H \mathbf{U}^H(\Delta \tau_{i,j_k}) \mathbf{S}_p^H \mathbf{F}^H(\Delta f_{i,j_k})\}. \end{aligned} \quad (12)$$

In the following, we aim to derive (12). To alleviate the pilot contamination, the distance among the slave APs that share the common pilot sequence should be as far as possible, resulting in severe path loss and lower received signal power. Furthermore, since the APs are deployed in relatively high positions, the APs can transmit signal without blockage issues. Based on these reasons, the pilot contamination from other clusters predominantly depends on the main path with path delay $\varsigma_{i,j_k}^0 = \frac{d_{i,j_k}}{c}$, $\forall i \in \{\mathcal{P}_p \setminus i_{j_k}^p\}$, where d_{i,j_k} is the distance between the i -th slave AP and the j_k -th master AP and c is the speed of light. For this special case, $\mathbf{U}(\Delta \tau_{i,j_k}) \in \mathbb{R}^{(M-N+1) \times 1}$ is a vector and $\mathbf{h}_{i,j_k} \in \mathbb{C}^{1 \times 1}$ is $\alpha_{i,j_k}^0 \sqrt{\beta_{i,j_k}} \psi_{i,j_k}^0$. Then, owing to the independent variables of $\mathbf{F}(\Delta f_{i,j_k})$ and $\mathbf{U}(\Delta \tau_{i,j_k})$, we have

$$\begin{aligned} & \text{var}\{\mathbf{F}(\Delta f_{i,j_k}) \mathbf{S}_p \mathbf{U}(\Delta \tau_{i,j_k}) \mathbf{h}_{i,j_k}\} \\ &= \alpha_{i,j_k}^0 \beta_{i,j_k} \mathbb{E}\left\{\mathbf{F}(\Delta f_{i,j_k}) \mathbf{S}_p \mathbb{E}\{\mathbf{U}(\Delta \tau_{i,j_k}) \mathbf{U}^H(\Delta \tau_{i,j_k})\} \mathbf{S}_p^H \mathbf{F}^H(\Delta f_{i,j_k})\right\}. \end{aligned} \quad (13)$$

Next, we derive the result of $\mathbb{E}\{\mathbf{U}(\Delta \tau_{i,j_k}) \mathbf{U}^H(\Delta \tau_{i,j_k})\}$, denoted as \mathbf{A} . Owing to the TO between the i -th slave AP and the j_k -th master AP, we have the following three cases.

Case 1: $0 \leq \Delta \tau_{i,j_k} < 1 - \frac{\varsigma_{i,j_k}^0}{T_s}$, we define $\bar{\mathbf{A}}(0) = \mathbf{U}(\Delta \tau_{i,j_k}) \mathbf{U}^H(\Delta \tau_{i,j_k})$ and have

$$\bar{\mathbf{A}}(0) = \mathbf{U}(\Delta \tau_{i,j_k}) \mathbf{U}^H(\Delta \tau_{i,j_k}) = [0, 1 - x_{i,j_k}^0, x_{i,j_k}^0, 0, \dots, 0]^T [0, 1 - x_{i,j_k}^0, x_{i,j_k}^0, 0, \dots, 0], \quad (14)$$

where x_{i,j_k}^0 is $x_{i,j_k}^0 = \Delta \tau_{i,j_k} + \frac{\varsigma_{i,j_k}^0}{T_s}$. As can be seen from (14), there are only four non-zero elements, which are denoted as

$$[\bar{\mathbf{A}}(0)]_{2,2} = (1 - x_{i,j_k}^0)^2, [\bar{\mathbf{A}}(0)]_{3,3} = (x_{i,j_k}^0)^2, [\bar{\mathbf{A}}(0)]_{2,3} = [\bar{\mathbf{A}}(0)]_{3,2} = (1 - x_{i,j_k}^0)(x_{i,j_k}^0). \quad (15)$$

Case 2: $v - 1 - \frac{\varsigma_{i,j_k}^0}{T_s} \leq \Delta \tau_{i,j_k} < v - \frac{\varsigma_{i,j_k}^0}{T_s}$, $\forall v \in \{2, \dots, \eta\}$, we denote $\mathbf{U}(\Delta \tau_{i,j_k}) \mathbf{U}^H(\Delta \tau_{i,j_k})$

as $\bar{\mathbf{A}}(v-1)$ and have

$$\begin{aligned}\bar{\mathbf{A}}(v-1) &= \mathbf{U}(\Delta\tau_{i,j_l}) \mathbf{U}^H(\Delta\tau_{i,j_l}) \\ &= \underbrace{[0, \dots, 0, v - x_{i,j_k}^0, x_{i,j_k}^0 + 1 - v, \dots]}_v \underbrace{[0, \dots, 0, v - x_{i,j_k}^0, x_{i,j_k}^0 + 1 - v, \dots]}_v.\end{aligned}\quad (16)$$

Similar to the result given in (15), there are only four non-zero elements, which are denoted as

$$\begin{aligned}[\bar{\mathbf{A}}(v-1)]_{v+1,v+1} &= (v - x_{i,j_k}^0)^2, [\bar{\mathbf{A}}(v-1)]_{v+2,v+2} = (x_{i,j_k}^0 + 1 - v)^2, \\ [\bar{\mathbf{A}}(v-1)]_{v+1,v+2} &= [\bar{\mathbf{A}}(v-1)]_{v+2,v+1} = (v - x_{i,j_k}^0)(x_{i,j_k}^0 + 1 - v).\end{aligned}\quad (17)$$

Case 3: $\eta - \frac{\varsigma_{i,j_k}^0}{T_s} \leq \Delta\tau_{i,j_k} < \eta$, we define $\bar{\mathbf{A}}(\eta - \frac{\varsigma_{i,j_k}^0}{T_s}) = \mathbf{U}(\Delta\tau_{i,j_k}) \mathbf{U}^H(\Delta\tau_{i,j_k})$ and have

$$\begin{aligned}\bar{\mathbf{A}}(\eta - \frac{\varsigma_{i,j_k}^0}{T_s}) &= \mathbf{U}(\Delta\tau_{i,j_k}) \mathbf{U}^H(\Delta\tau_{i,j_k}) \\ &= \underbrace{[0, \dots, \eta + 1 - x_{i,j_k}^0, x_{i,j_k}^0 - \eta, \dots]}_{\eta+1} \underbrace{[0, \dots, \eta + 1 - x_{i,j_k}^0, x_{i,j_k}^0 - \eta, \dots]}_{\eta+1}.\end{aligned}\quad (18)$$

The non-zero elements of $\bar{\mathbf{A}}(\eta - \frac{\varsigma_{i,j_k}^0}{T_s})$ are given by

$$\begin{aligned}[\bar{\mathbf{A}}(\eta - \frac{\varsigma_{i,j_k}^0}{T_s})]_{\eta+2,\eta+2} &= (\eta + 1 - x_{i,j_k}^0)^2, [\bar{\mathbf{A}}(\eta - \frac{\varsigma_{i,j_k}^0}{T_s})]_{\eta+3,\eta+3} = (x_{i,j_k}^0 - \eta)^2, \\ [\bar{\mathbf{A}}(\eta - \frac{\varsigma_{i,j_k}^0}{T_s})]_{\eta+2,\eta+3} &= [\bar{\mathbf{A}}(\eta - \frac{\varsigma_{i,j_k}^0}{T_s})]_{\eta+3,\eta+2} = (\eta + 1 - x_{i,j_k}^0)(x_{i,j_k}^0 - \eta).\end{aligned}\quad (19)$$

By using the integration and the above results, $\mathbb{E}\{\mathbf{U}(\Delta\tau_{i,j_k}) \mathbf{U}^H(\Delta\tau_{i,j_k})\}$ is given by

$$\mathbf{A} = \mathbb{E}\{\mathbf{U}(\Delta\tau_{i,j_k}) \mathbf{U}^H(\Delta\tau_{i,j_k})\} = \mathbb{E}\{\bar{\mathbf{A}}(0) + \sum_{v=2}^{\eta} \bar{\mathbf{A}}(v-1) + \bar{\mathbf{A}}(\eta - \frac{\varsigma_{i,j_k}^0}{T_s})\}.\quad (20)$$

Based on these discussions, if $\eta > 1$, the elements of \mathbf{A} are given by

$$[\mathbf{A}]_{2,2} = \frac{(1 - \frac{\varsigma_{i,j_k}^0}{T_s})^3}{3\eta}, [\mathbf{A}]_{2,3} = [\mathbf{A}]_{3,2} = \frac{1 - 3\left(\frac{\varsigma_{i,j_k}^0}{T_s}\right)^2 + 2\left(\frac{\varsigma_{i,j_k}^0}{T_s}\right)^3}{6\eta},\quad (21)$$

$$[\mathbf{A}]_{3,3} = \frac{2 - \left(\frac{\varsigma_{i,j_k}^0}{T_s}\right)^3}{3\eta}, [\mathbf{A}]_{v+1,v+2} = [\mathbf{A}]_{v+2,v+1} = \frac{1}{6\eta}, \forall v \in \{2, \dots, \eta\},\quad (22)$$

$$[\mathbf{A}]_{v+2,v+2} = \frac{2}{3\eta}, \forall v \in \{2, \dots, \eta - 1\},\quad (23)$$

$$[\mathbf{A}]_{\eta+2,\eta+2} = \frac{2 - \left(1 - \frac{\varsigma_{i,j_k}^0}{T_s}\right)^3}{3\eta}, [\mathbf{A}]_{\eta+2,\eta+3} = [\mathbf{A}]_{\eta+3,\eta+2} = \frac{3\left(\frac{\varsigma_{i,j_k}^0}{T_s}\right)^2 - 2\left(\frac{\varsigma_{i,j_k}^0}{T_s}\right)^3}{6\eta}, \quad (24)$$

$$[\mathbf{A}]_{\eta+3,\eta+3} = \frac{\left(\frac{\varsigma_{i,j_k}^0}{T_s}\right)^3}{3\eta}. \quad (25)$$

For the special case of $\eta = 1$, the $[3, 3]$ -th element of \mathbf{A} is different from the result given in (22), which is given by

$$[\mathbf{A}]_{3,3} = \frac{1 - 3\left(\frac{\varsigma_{i,j_k}^0}{T_s}\right)^2 + 3\frac{\varsigma_{i,j_k}^0}{T_s}}{3}. \quad (26)$$

Then, since the $[n, m]$ -th element of $\mathbf{F}(\Delta f_{i,j_k}) \mathbf{S}_p$ is $e^{j2\pi(n-1)\Delta f_{i,j_k} T_s} s_p^{n-m}$, we have

$$\begin{aligned} [\mathbf{F}(\Delta f_{i,j_k}) \mathbf{S}_p \mathbb{E}\{\mathbf{U}(\Delta \tau_{i,j_k}) \mathbf{U}^H(\Delta \tau_{i,j_k})\}]_{n,m} &= \sum_{k'=1}^{M-N+1} [\mathbf{F}(\Delta f_{i,j_k}) \mathbf{S}_p]_{n,k'} [\mathbf{A}]_{k',m} \\ &= \sum_{k'=m-1}^{m+1} [\mathbf{A}]_{k',m} e^{j2\pi(n-1)\Delta f_{i,j_k} T_s} s_p^{n-k'}, \end{aligned} \quad (27)$$

where $s_p^{n-k'}$ is 0 when $n - k' < 0$ and $n - k' > N - 1$.

By substituting the result of (27) into (13), we have

$$\begin{aligned} &[\mathbf{F}(\Delta f_{i,j_k}) \mathbf{S}_p \mathbb{E}\{\mathbf{U}(\Delta \tau_{i,j_k}) \mathbf{U}^H(\Delta \tau_{i,j_k})\} \mathbf{S}_p^H \mathbf{F}^H(\Delta f_{i,j_k})]_{n,m} \\ &= \sum_{k'=1}^{M-N+1} [\mathbf{F}(\Delta f_{i,j_k}) \mathbf{S}_p \mathbb{E}\{\mathbf{U}(\Delta \tau_{i,j_k}) \mathbf{U}^H(\Delta \tau_{i,j_k})\}]_{n,k'} [\mathbf{S}_p^H \mathbf{F}^H(\Delta f_{i,j_k})]_{k',m} \\ &= \sum_{k'=1}^{M-N+1} \sum_{k_1=k'-1}^{k'+1} [\mathbf{A}]_{k_1,k'} e^{j2\pi(n-1)\Delta f_{i,j_k} T_s} s_p^{n-k_1} e^{-j2\pi(m-1)\Delta f_{i,j_k} T_s} s_p^{m-k'} \\ &= \sum_{k'=2}^{M-N+1} \sum_{k_1=k'-1}^{k'+1} [\mathbf{A}]_{k_1,k'} e^{j2\pi(n-m)\Delta f_{i,j_k} T_s} s_p^{n-k_1} s_p^{m-k'}. \end{aligned} \quad (28)$$

Then, based on the integration of CFO $\Delta f_{i,j_k}$, we have

$$\int_{-f_{\max}}^{f_{\max}} \frac{e^{j2\pi(n-m)\Delta f_{i,j_k} T_s}}{2f_{\max}} d\Delta f_{i,j_k} = \begin{cases} 1, & m = n \\ 0, & m \neq n. \end{cases} \quad (29)$$

As a result, $\text{var}\{\mathbf{F}(\Delta f_{i,j_k}) \mathbf{S}_p \mathbf{U}(\Delta \tau_{i,j_k}) \mathbf{h}_{i,j_k}\}$ is a diagonal matrix, denoted as \mathbf{D}_{i,j_k} , whose

$[n, n]$ -th element can be expressed as

$$\begin{aligned} [\mathbf{D}_{i,j_k}]_{n,n} &\triangleq [\text{var}\{\mathbf{F}(\Delta f_{i,j_k}) \mathbf{S}_p \mathbf{U}(\Delta \tau_{i,j_k}) \mathbf{h}_{i,j_k}\}]_{n,n} \\ &= \alpha_{i,j_k}^0 \beta_{i,j_k} \sum_{k'=2}^{M-N+1} \sum_{k_1=k'-1}^{k'+1} [\mathbf{A}]_{k_1,k'} s_p^{n-k_1} s_p^{n-k'}. \end{aligned} \quad (30)$$

By substituting (30) into (13), we obtain Ξ , which can be written as

$$\Xi = \sum_{i \in \{\mathcal{P}_p \setminus i_{j_k}^p\}} \mathbf{D}_{i,j_k} + \sigma^2 \mathbf{I}_M. \quad (31)$$

In the following, we derive the partial derivatives of $\boldsymbol{\theta}$. Define $\mathbf{M} = \text{diag}(0, 1, \dots, M)$ and let $\mathbf{e}_l^{i_{j_k}^p, j_k}$ denote the l -th column of unit matrix $\mathbf{I}_{L_{i_{j_k}^p, j_k}}$. Denote $\mathbf{U}'(\Delta \tau_{i_{j_k}^p, j_k})$ as the partial derivation with respect to $\Delta \tau_{i_{j_k}^p, j_k}$, whose l -th column has two non-zeros elements equal to -1 at component $\left[1 + \frac{\Delta \tau_{i_{j_k}^p, j_k}}{T_s} + \frac{s_{i_{j_k}^p, j_k}^l}{T_s}\right]$ and equal to 1 at component $1 + \left[1 + \frac{\Delta \tau_{i_{j_k}^p, j_k}}{T_s} + \frac{s_{i_{j_k}^p, j_k}^l}{T_s}\right]$. Based on these definitions, we have

$$\frac{\partial \mathbf{m}(\boldsymbol{\theta})}{\partial \theta_1} = \mathbf{F}(\Delta f_{i_{j_k}^p, j_k}) \mathbf{S}_p \mathbf{U}'(\Delta \tau_{i_{j_k}^p, j_k}) \mathbf{h}_{i_{j_k}^p, j_k}, \quad (32)$$

$$\frac{\partial \mathbf{m}(\boldsymbol{\theta})}{\partial \theta_2} = j2\pi \mathbf{M} \mathbf{F}(\Delta f_{i_{j_k}^p, j_k}) \mathbf{S}_p \mathbf{U}(\Delta \tau_{i_{j_k}^p, j_k}) \mathbf{h}_{i_{j_k}^p, j_k}, \quad (33)$$

$$\frac{\partial \mathbf{m}(\boldsymbol{\theta})}{\partial \theta_{2l+3}} = \mathbf{F}(\Delta f_{i_{j_k}^p, j_k}) \mathbf{S}_p \mathbf{U}(\Delta \tau_{i_{j_k}^p, j_k}) \mathbf{h}_{i_{j_k}^p, j_k} \mathbf{e}_l^{i_{j_k}^p, j_k}, \forall l \in \{0, 1, \dots, L_{i_{j_k}^p, j_k}\}, \quad (34)$$

$$\frac{\partial \mathbf{m}(\boldsymbol{\theta})}{\partial \theta_{2l+4}} = j \mathbf{F}(\Delta f_{i_{j_k}^p, j_k}) \mathbf{S}_p \mathbf{U}(\Delta \tau_{i_{j_k}^p, j_k}) \mathbf{h}_{i_{j_k}^p, j_k} \mathbf{e}_l^{i_{j_k}^p, j_k}, \forall l \in \{0, 1, \dots, L_{i_{j_k}^p, j_k}\}. \quad (35)$$

Finally, by defining the $M \times 2(L_{i_{j_k}^p, j_k} + 1)$ matrix $\boldsymbol{\Omega} = \left[\frac{\partial \mathbf{m}(\boldsymbol{\theta})}{\partial \theta_1}, \frac{\partial \mathbf{m}(\boldsymbol{\theta})}{\partial \theta_2}, \dots, \frac{\partial \mathbf{m}(\boldsymbol{\theta})}{\partial \theta_{2L_{i_{j_k}^p, j_k} + 2}}\right]$, the Fisher matrix can be written as

$$\mathbf{J}(\boldsymbol{\theta}) = 2\text{Re}\{\boldsymbol{\Omega}^H \Xi \boldsymbol{\Omega}\}. \quad (36)$$

Finally, the CRBs of CFO and TO are obtained by the first two diagonal elements of $\mathbf{J}^{-1}(\boldsymbol{\theta})$. These CRBs can be regarded as the theoretical lower bound of mean square errors (MSEs) between the real parameters and estimated results. Furthermore, as given the result in (36), it is worth emphasizing that the estimation accuracy is strongly related to the pilot contamination, especially for the low noise power regime.

B. Maximum Likelihood Estimation

In this subsection, we jointly estimate CFO and TO between the $i_{j_k}^p$ slave AP and the j_k -th master AP, assuming that the noise power σ^2 and the path delays $\zeta_{i_{j_k}^p, j_k}^l, \forall l \in \{0, 1, 2, \dots, L_{i_{j_k}^p, j_k} - 1\}$ are known⁴. Then, the ML estimation can be obtained by minimizing the square distance, which is given by

$$\left\| \mathbf{y}_{j_k} - \mathbf{F} \left(\Delta f_{i_{j_k}^p, j_k} \right) \mathbf{S}_p \mathbf{U} \left(\Delta \tau_{i_{j_k}^p, j_k} \right) \mathbf{h}_{i_{j_k}^p, j_k} \right\|^2. \quad (37)$$

For given $\frac{\Delta \tau_{i_{j_k}^p, j_k}}{T_s}$ and $\Delta f_{i_{j_k}^p, j_k} T_s$, the estimation of $\mathbf{h}_{i_{j_k}^p, j_k}$ can be obtained by

$$\begin{aligned} \hat{\mathbf{h}}_{i_{j_k}^p, j_k} &= \left(\mathbf{U}^H \left(\Delta \tau_{i_{j_k}^p, j_k} \right) \mathbf{S}_p^H \mathbf{F}^H \left(\Delta f_{i_{j_k}^p, j_k} \right) \mathbf{F} \left(\Delta f_{i_{j_k}^p, j_k} \right) \mathbf{S}_p \mathbf{U} \left(\Delta \tau_{i_{j_k}^p, j_k} \right) \right)^{-1} \\ &\times \mathbf{U}^H \left(\Delta \tau_{i_{j_k}^p, j_k} \right) \mathbf{S}_p^H \mathbf{F}^H \left(\Delta f_{i_{j_k}^p, j_k} \right) \mathbf{y}_{j_k}. \end{aligned} \quad (38)$$

Then, by substituting the result of (38) into (37), we can estimate $\Delta f_{i_{j_k}^p, j_k} T_s$ and $\frac{\Delta \tau_{i_{j_k}^p, j_k}}{T_s}$ by maximizing the following quadratic form

$$\begin{aligned} &\mathbf{y}_{j_k} \mathbf{F} \left(\Delta f_{i_{j_k}^p, j_k} \right) \mathbf{S}_p \mathbf{U} \left(\Delta \tau_{i_{j_k}^p, j_k} \right) \left(\mathbf{U}^H \left(\Delta \tau_{i_{j_k}^p, j_k} \right) \mathbf{S}_p^H \mathbf{F}^H \left(\Delta f_{i_{j_k}^p, j_k} \right) \mathbf{F} \left(\Delta f_{i_{j_k}^p, j_k} \right) \mathbf{S}_p \mathbf{U} \left(\Delta \tau_{i_{j_k}^p, j_k} \right) \right)^{-1} \\ &\times \mathbf{U}^H \left(\Delta \tau_{i_{j_k}^p, j_k} \right) \mathbf{S}_p^H \mathbf{F}^H \left(\Delta f_{i_{j_k}^p, j_k} \right) \mathbf{y}_{j_k}. \end{aligned} \quad (39)$$

This can be regarded as maximizing the energy of the projection \mathbf{y}_{j_k} onto the column space of the signal matrix $\mathbf{F} \left(\Delta f_{i_{j_k}^p, j_k} \right) \mathbf{S}_p \mathbf{U} \left(\Delta \tau_{i_{j_k}^p, j_k} \right)$. As a result, the ML estimator is obtained by searching over a two-dimensional sufficiently fine grid of points with respect to the variables $\Delta f_{i_{j_k}^p, j_k} T_s$ and $\frac{\Delta \tau_{i_{j_k}^p, j_k}}{T_s}$.

IV. SYNCHRONIZATION BASED ON PILOT ASSIGNMENT

Based on the result given in (36), we devise a synchronization scheme based on pilot sharing to minimize the sum of CRBs while simultaneously satisfying the requirement for all APs with limited overhead.

⁴Due to the fact that the $i_{j_k}^p$ -th slave AP and the j_k -th master AP are in the same cluster, the distances from the $i_{j_k}^p$ -th slave AP to the j_k -th master AP is closer than that of the slave APs in other clusters and the variation of multi-path delay is relatively slow compared to inter-cluster ones. Furthermore, since the synchronization is performed periodically in a short time interval and all APs are deployed in high locations with relatively stable propagation paths, these factors lead to the known path delays.

A. Problem Formulation

In this subsection, we jointly optimize the cluster classification, pilot overhead, and pilot sharing scheme to minimize the synchronization errors. By denoting the synchronization requirement of the i -th slave AP and the j_k -th master AP as $\text{CRB}_{i,j_k}^{\text{Req}}$, $j_k \in \mathcal{C}_k$, $\forall i \in \{\mathcal{C}_k \setminus j_k\}$, $k = \{1, \dots, K_C\}$, the minimization of sum CRBs can be formulated as

$$\begin{aligned} \min_{K_C, \mathcal{C}_k, k \in \{1, \dots, K_C\}, \tau, \mathcal{P}_p, p \in \{1, \dots, \tau\}} & \sum_{k=1}^{K_C} \sum_{i \in \{\mathcal{C}_k \setminus j_k\}} \text{CRB}_{i,j_k}(\Delta f_{i,j_k}, \Delta \tau_{i,j_k}) \\ \text{s. t.} & \text{CRB}_{i,j_k}(\Delta f_{i,j_k}, \Delta \tau_{i,j_k}) \leq \text{CRB}_{i,j_k}^{\text{Req}}, \\ & j_k \in \mathcal{C}_k, \forall i \in \{\mathcal{C}_k \setminus j_k\}, k \in \{1, \dots, K_C\}, \end{aligned} \quad (40a)$$

$$2K_C + \tau \leq L_S, \quad (40b)$$

where $\text{CRB}_{i,j_k}(\Delta f_{i,j_k}, \Delta \tau_{i,j_k})$ is the theoretical lower bound for estimation errors of CFO and TO between the i -th slave AP and the j_k master AP, τ is the pilot overhead, and L_S is the total overhead for synchronization. Constraint (40a) means that each AP should satisfy the minimal requirements for synchronization, and constraint (40b) represents that the total overhead, including the pilot overhead and information exchange, should be less than L_S .

As can be seen from (40), the synchronization performance will be better if there are more master APs and only one slave AP. However, it is unrealistic to deploy more master APs and only one slave AP in the cell-free mMIMO systems, which leads to significant overhead for exchanging information and impractical implementation. Furthermore, considering the limited channel resources and high requirements of synchronization, it is challenging to strike a balance between the synchronization performance and overhead, i.e., information exchange and pilot overhead. To address this issue, we aim to devise a synchronization scheme with low overhead while simultaneously satisfying the requirements of each AP.

To address this NP-hard problem, we first need to classify the clusters according to APs' synchronization requirements, and then allocate the pilot sequences to all slave APs. Therefore, Problem (40) can be simplified into two sub-problems, including adaptive cluster classification problem and pilot sharing scheme, which is depicted in Fig. 2.

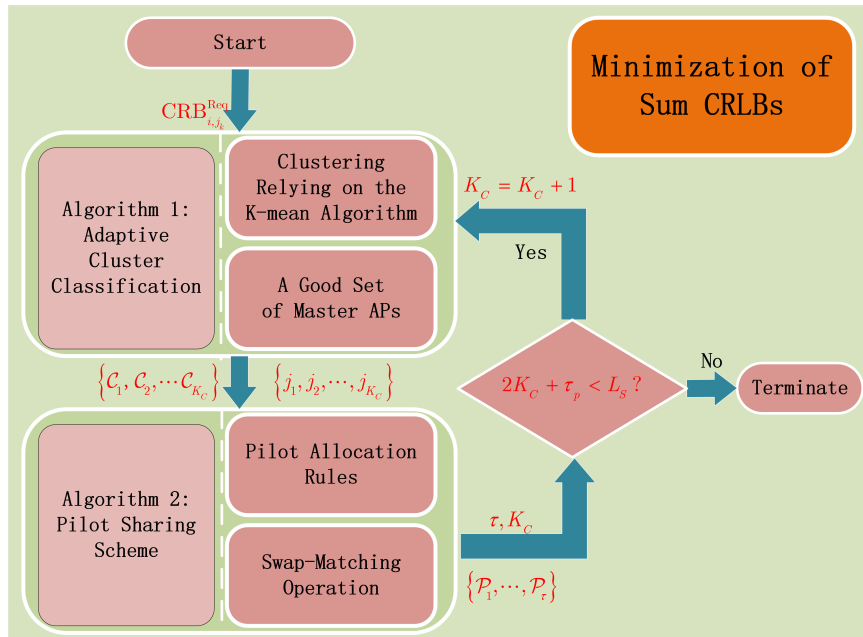


Fig. 2: Illustration for solving the sum of CRBs.

B. Adaptive Cluster Classification

In this subsection, we find a good way to classify the clusters with a good set of master APs while considering the overhead of information exchange. By ignoring the pilot allocation strategy, Problem (40) can be simplified into

$$\min_{K_C, \mathcal{C}_k, k \in \{1, \dots, K_C\}} \sum_{k=1}^{K_C} \sum_{i \in \{\mathcal{C}_k \setminus j_k\}} \text{CRB}_{i,j_k}(\Delta f_{i,j_k}, \Delta \tau_{i,j_k})$$

$$\text{s. t.} \quad \text{CRB}_{i,j_k}(\Delta f_{i,j_k}, \Delta \tau_{i,j_k}) \leq \text{CRB}_{i,j_k}^{\text{Req}},$$

$$j_k \in \mathcal{C}_k, \forall i \in \{\mathcal{C}_k \setminus j_k\}, l \in \{1, \dots, K_C\}, \quad (41a)$$

$$2K_C < L_S. \quad (41b)$$

Obviously, minimizing the sum of CRBs can be obtained by simply having one slave AP with the largest path gain, but this violates the constraint (41b) owing to the heavy burden on information exchange. Conversely, deploying an insufficient number of clusters may increase the average distance between master AP and slave APs in each cluster, which leads to a significant decrease in synchronization performance. Furthermore, even though the clusters are classified, it is still worth exploring which AP can be chosen as the master AP to minimize the CRB. To address these

issues, an adaptive cluster classification based on the synchronization requirements is proposed, and a criterion that finds a good set of master APs is to minimize the sum of CRBs.

In the following, our first step is to investigate how to find a reasonable number of clusters according to the stringent synchronization performance. Since estimation errors decrease with the signal-to-noise ratio (SNR) (dB) [17], the synchronization performance can be transformed into the requirement of signal-to-interference-plus-noise ratio (SINR) (dB) by treating the pilot contamination as a part of the noise, which can be expressed as

$$\text{CRB}_{i,j_k}(\Delta f_{i,j_k}, \Delta \tau_{i,j_k}) \leq \text{CRB}_{i,j_k}^{\text{Req}} \Rightarrow \text{SINR}_{i,j_k} \geq \text{SINR}_{i,j_k}^{\text{Req}}. \quad (42)$$

Then, based on the required SINR, we derive the size of each cluster, which can be used to determine the number of clusters. Specifically, the maximum intra-cluster distance can be found by relying on the relationship between the distance and path loss. For the ideal case, i.e., no multiple paths and no pilot contamination, the expectation of ideal SINR can be written as

$$\text{SINR}^{\text{ideal}} = 10 \log_{10} \left(\frac{\text{Tr}\{\mathbf{D}^{\text{ideal}}\}}{M\sigma^2} \right), \quad (43)$$

where $\mathbf{D}^{\text{ideal}}$ is $\text{var}\left\{\mathbf{F}(\Delta f_{i,j_k}^p) \mathbf{S}_p \mathbf{U}(\Delta \tau_{i,j_k}^p) \mathbf{h}_{i,j_k}^p\right\}$, whose proof is omitted owing to the same derivation of (30). Then, the maximum intra-cluster distance is determined by the minimum $\text{MSE}_{i,j_k}^{\text{Req}}, \forall i \in \{\mathcal{C}_k \setminus j_k\}, \forall k \in \{1, \dots, K_C\}$. For ease of expression, we denote the SINR^{min} as the equivalent condition of the minimum $\text{MSE}_{i,j_k}^{\text{Req}}$. By assuming that α_{i,j_k}^0 is 1 and substituting (43) into (42), we have

$$\text{SINR}^{\text{ideal}} \geq \text{SINR}^{\text{min}} \Rightarrow \beta^{\text{min}} \geq \frac{M\sigma^2 10^{\frac{\text{SINR}^{\text{min}}}{10}}}{\text{Tr}\left\{\mathbb{E}\left\{\mathbf{F}(\Delta f_{i,j_k}^p) \mathbf{S}_p \mathbf{A} \mathbf{S}_p^H \mathbf{F}^H(\Delta f_{i,j_k}^p)\right\}\right\}}. \quad (44)$$

By using the three-slope channel model given in [2], the maximum intra-cluster distance can be readily obtained by

$$\text{dis}^{\text{max}} = 10^{-\frac{2}{7} \log \frac{M\sigma^2 10^{\frac{\text{SINR}^{\text{min}}}{10}}}{\text{Tr}\left\{\mathbb{E}\left\{\mathbf{F}(\Delta f_{i,j_k}^p) \mathbf{S}_p \mathbf{A} \mathbf{S}_p^H \mathbf{F}^H(\Delta f_{i,j_k}^p)\right\}\right\}} - \frac{L^{\text{loss}}}{35}}, \quad (45)$$

where L^{loss} is the constant factor. Although we cannot directly determine the number of clusters, we can use this maximum intra-cluster distance to determine whether the clusters satisfy the synchronization requirements.

Based on the above discussions, for a fixed number of cluster K_C , the minimum sum of CRBs can be obtained by maximizing the sum of SINRs, which can be expressed as

$$\begin{aligned} & \max_{\mathcal{C}_k, k \in \{1, \dots, K_C\}} \sum_{k=1}^{K_C} \sum_{i \in \{\mathcal{C}_k \setminus j_k\}} \text{SINR}_{i, j_k} \\ & \text{s. t.} \quad \text{SINR}_{i, j_k} \geq \text{SINR}_{i, j_k}^{\text{Req}}, j_k \in \mathcal{C}_k, \forall i \in \{\mathcal{C}_k \setminus j_k\}, k \in \{1, \dots, K_C\}, \end{aligned} \quad (46a)$$

$$2K_C < L_S. \quad (46b)$$

Although it is impossible to derive a closed-form expression of SINR_{i, j_k} , the result of the pilot contamination reveals that the power primarily depends on distance-based large-scale fading factors. Consequently, the maximum sum of SINRs can be obtained by shortening the distance between the slave AP and master AP. Then, the cluster can be classified by minimizing the sum of intra-cluster distances while ensuring that the AP-to-centroid distance in the cluster is no larger than the maximum intra-cluster distance dis^{\max} , which can be written as

$$\begin{aligned} & \min_{K_C, \mathcal{C}_1, \dots, \mathcal{C}_{K_C}} \sum_{k=1}^{K_C} \sum_{i \in \mathcal{C}_k} |(x_k, y_k) - \text{Loc}_i|, \\ & \text{s. t.} \quad |(x_k, y_k) - \text{Loc}_i| \leq \text{dis}^{\max}, \forall i \in \mathcal{C}_k, k \in \{1, \dots, K_C\}, \end{aligned} \quad (47a)$$

where (x_k, y_k) means the optimal 2-dimensional location of the k -th cluster's centroid that has the minimal sum of distances to all APs in the k -th cluster, and Loc_i is the 2-dimensional location of the i -th AP. However, for the given number of clusters K_C , it is still challenging to obtain the optimal solution of Problem (47) since it is an the NP-hard problem. To address this issue, we classify the clusters by using the K-means algorithm, whose details are given in [26]. By combining the K-means algorithm with the maximum intra-cluster distance, we can gradually classify the clusters by gradually increasing the number of clusters K_C until the maximum intra-cluster distances of all clusters are no more than the value given in (45).

Based on the given clusters, a good set of master APs should be found to minimize the sum of CRBs. Similar to the clustering approach, the master AP and the centroid of the cluster should have the same characteristics, thereby maximizing the sum of path gains in the cluster and improving the synchronization performance. Mathematically, a criteria that finds a good set

Algorithm 1 Adaptive Cluster Classification based on K-means Algorithm

- 1: Initialize the iterative number $n = 1$ and the number of clusters $K_C^n = 2$;
 - 2: Initialize the cluster based on the K-means algorithm and find the set of master APs.
 - 3: Calculate the maximum intra-cluster distance between the master AP and the slave AP of each cluster, denoted as $\text{dis}_{k,n}^{\max}, \forall k \in \{1, \dots, K_C^n\}$;
 - 4: **while** $(\min \{ \text{dis}_{1,n}^{\max}, \dots, \text{dis}_{K_C^n,n}^{\max} \} > \text{dis}^{\max})$ **do**
 - 5: Update $n = n + 1, K_C^n = K_C^{n-1} + 1$;
 - 6: Update the cluster classification $\mathcal{C}^n = \{ \mathcal{C}_1^n \cup \dots \mathcal{C}_{K_C^n}^n \}$ with K_C^n , by using the K-means algorithm;
 - 7: Find the set of master APs by using (48);
 - 8: Calculate the maximum intra-cluster distance between the master AP and the slave AP of each cluster, denoted as $\text{dis}_{k,n}^{\max}, \forall k \in \{1, \dots, K_C^n\}$;
 - 9: **end while**
-

of master APs can be written as

$$j_k = \arg \min_{j_k \in \mathcal{C}_k} \left\{ \sum_{i \in \{\mathcal{C}_k \setminus j_k\}} \|\text{Loc}_{j_k} - \text{Loc}_i\| \right\}, \forall k \in \{1, \dots, K_C\}. \quad (48)$$

By using this criterion of (48), the master AP has the minimum sum distances to all slave APs, which leads to larger path gain and better synchronization performance.

Based on the above discussions, we propose an adaptive cluster classification based on the K-means algorithm, which is detailed in Algorithm 1. Initially, we divide all APs in this area into K_C clusters and find the maximum intra-cluster distance between the master AP and the slave AP of each cluster. Then, if the maximum inter-cluster distance of all clusters is less than the defined value dis^{\max} , the adaptive cluster classification based on the K-means algorithm terminates. Otherwise, the number of clusters will increase by 1, and then the clusters will be classified again until the maximum intra-cluster distances of all clusters are less than the specific value dis^{\max} .

C. Pilot Sharing Algorithm

Based on the given cluster $\mathcal{C}_k, \forall k \in \{1, \dots, K_C\}$, we jointly optimize the pilot overhead τ and the pilot sharing scheme, $\mathcal{P}_p, \forall p \in \{1, \dots, \tau\}$, to minimize the estimation errors. Mathematically,

minimizing the sum of CRBs can be expressed as

$$\begin{aligned} \min_{\tau, \mathcal{P}_p, p \in \{1, \dots, \tau\}} \quad & \sum_{k \in \{1, 2, \dots, K_C\}} \sum_{i \in \{\mathcal{C}_k \setminus j_k\}} \text{CRB}_{i, j_k}(\Delta f_{i, j_k}, \Delta \tau_{i, j_k}) \\ \text{s. t.} \quad & \text{CRB}_{i, j_k}(\Delta f_{i, j_k}, \Delta \tau_{i, j_k}) \leq \text{CRB}_{i, j_k}^{\text{Req}}, \\ & j_k \in \mathcal{C}_k, \forall i \in \{\mathcal{C}_k \setminus j_k\}, k \in \{1, \dots, K_C\}, \end{aligned} \quad (49a)$$

$$\tau \leq L_S - 2K_C. \quad (49b)$$

As can be seen from (49), the optimal solution can be obtained if all slave APs are allocated unique pilot sequences. However, this orthogonal pilot strategy is impractical owing to significant pilot overhead. To address this issue, we devise a pilot-sharing scheme by searching for the optimal solution with the given clusters.

In the following, we first simplify the pilot-sharing scheme by transforming it into a graph coloring problem. Specifically, two rules are defined to share the pilot sequence. For the first rule, to reduce the pilot contamination, the slave APs in the common cluster cannot share the same pilot sequence, which can be formulated as

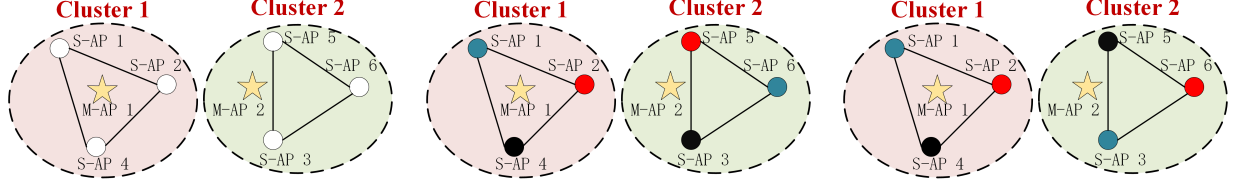
$$\mathbf{s}_p^H \mathbf{s}_{p'} = 0, \quad \forall i^p \quad \text{and} \quad \forall i^{p'} \in \mathcal{C}_k, \quad \forall k \in \{1, \dots, K_C\}, \quad \text{and} \quad i^p \neq i^{p'}, \quad (50)$$

where $\mathbf{s}_p \in \mathbb{C}^{N \times 1}$ is the orthogonal pilot sequence allocated to the i^p -th slave AP. By denoting $\mathcal{S} = \mathcal{S}_1 \cup \mathcal{S}_2 \cdots \mathcal{S}_{K_C}$, we define a binary matrix $\mathbf{B} \in \mathbb{N}^{|\mathcal{S}| \times |\mathcal{S}|}$, where $|\mathcal{S}|$ denotes the number of element in \mathcal{S} , to indicate whether the i -th device is a potential candidate for sharing the common pilot sequence with the i' -th device. The i -th row and i' -th column element of the matrix \mathbf{B} is given by

$$b_{i, i'} = \begin{cases} 1, & i \cup i' \notin \mathcal{C}_k, \forall k \in \{1, \dots, K_C\}, \text{ and } i \neq i' \\ 0, & \text{otherwise,} \end{cases} \quad (51)$$

$b_{i, i'} = 1$ means that the i -th slave AP and the i' -th slave AP are in a common cluster, and thus these two APs should be allocated unique orthogonal pilot sequences. By contrast, $b_{i, i'} = 0$ denotes that the i' -th slave and i -th slave AP belong to different clusters, and it is possible to share the common pilot sequence between the i -th slave AP and the i' -th slave AP.

The second rule is to allocate the pilot sequence in a fair manner. Specifically, the p -th pilot



(a) Undirected graph based on given clusters, where S-AP and M-AP represent the slave AP and master AP, respectively.

(b) Pilot assignment based on the Dsaturn algorithm, where the same color indicates that the same pilot sequence is used.

(c) Pilot allocation after combining the Dsaturn algorithm with the swap-matching operation.

Fig. 3: Undirected graph and pilot allocation schemes.

sequence can only be reused no more than N^{\max} times, which can be written as

$$|\mathcal{P}_p| \leq N^{\max}, \forall p \in \{1, \dots, \tau\}. \quad (52)$$

In this way, the worst-case scenario where a single pilot sequence is reused by too many devices can be avoided.

By using the above two rules, allocating the pilot sequence can be transformed into the graph coloring problem, which can be effectively solved by using the Dsaturn algorithm [27]. As depicted in Fig. 3, it is worth noting that a pilot allocation strategy based on the Dsaturn algorithm can follow the above two rules by using the lowest pilot overhead. However, this algorithm did not consider the estimation errors. For example, based on the result given in (30), the synchronization performance based on the pilot allocation strategy given in Fig. 3 (b) is not optimal, as slave AP 5 and slave AP 2 that share the same pilot sequence are in close proximity, which leads to severe pilot contamination and poor synchronization performance. Therefore, the objective function given in (49) cannot be minimized by simply using the Dsaturn algorithm. To address this issue, we introduce the switch matching and two-sided exchange into our pilot sharing scheme.

In the following, we introduce the concept of the swap-matching operation.

Definition 1: Given the pilot sharing scheme $\mathcal{P} = \{\mathcal{P}_1, \dots, \mathcal{P}_\tau\}$ with $i \in \mathcal{P}_n$, $i' \in \mathcal{P}_m$, and $i \notin \mathcal{P}_m$, $i' \notin \mathcal{P}_n$, a swap-matching $\mu_{i,i'}$ is defined by the function $\mathcal{P}_n(\mu_{i,i'}) = \mathcal{P}_n \setminus i \cup i'$ and $\mathcal{P}_m(\mu_{i,i'}) = \mathcal{P}_m \setminus i' \cup i$, and the exchanged pilot sharing scheme is defined as $\mathcal{P}_{\mu_{i,i'}} = \{\mathcal{P}_1, \dots, \mathcal{P}_n(\mu_{i,i'}), \mathcal{P}_m(\mu_{i,i'}), \mathcal{P}_\tau\}$.

To be more specific, the swap-matching means a matching generated by swap operation ⁵, in which two slave APs using different pilot sequences switch their pilot sequences while keeping all other pilot allocation assignments the same.

However, considering the previously defined two rules, the swap operation may not be allowed by all slave APs. Specifically, after this swap-matching operation, if the common pilot sequence is shared by the slave APs in the same cluster, then this operation is not permitted, which is detailed in the following.

Definition 2: Given the pilot sharing scheme $\{\mathcal{P}_1, \dots, \mathcal{P}_\tau\}$ with $i \in \mathcal{P}_n$, $i' \in \mathcal{P}_m$, and $i \notin \mathcal{P}_m$, $i' \notin \mathcal{P}_n$, a swap-blocking pair (i, i') satisfies that:

$$(1): \exists a, b \in \mathcal{P}_m(\mu_{i,i'}) \text{ or } \exists a, b \in \mathcal{P}_n(\mu_{i,i'}), a \cup b \in \mathcal{C}_k, \forall k \in \{1, \dots, K_C\}.$$

Compared to the conventional swap-blocking pair, we do not care whether this swap-matching operation, in which all slave APs are involved, is two-sided exchange-stable. This is due to the fact that the two-sided exchange-stable match can only converge to the locally optimal pilot sharing scheme ⁶. To search the globally optimal matching with the given pilot overhead τ , a swap-matching operation based on a simulated annealing method is proposed. Specifically, we will determine whether to update the pilot sharing scheme with a probability P_a , which is given by

$$P_a = \frac{1}{1 + e^{-T \times [\text{Obj}(\mathcal{P}_{\mu_{i,i'}}) - \text{Obj}(\mathcal{P}_\mu)]}}, \quad (53)$$

where T is a probability parameter. $\text{Obj}(\mathcal{P}_{\mu_{i,i'}})$ is denoted as the sum of SINR based on the given pilot sharing scheme $\mathcal{P}_{\mu_{i,i'}}$, which can be written as

$$\text{Obj}(\mathcal{P}_{\mu_{i,i'}}) = \begin{cases} \sum_{k \in \{1, \dots, K_C\}} \sum_{i_1 \in \{\mathcal{C}_k \setminus j_k\}} \text{SINR}_{i_1, j_k}, & \text{SINR}_{i_1, j_k} \geq \text{SINR}_{i_1, j_k}^{\text{Req}} \\ 0, & \text{SINR}_{i_1, j_k} < \text{SINR}_{i_1, j_k}^{\text{Req}}. \end{cases} \quad (54)$$

As can be seen from the probability in (53), if the swapped pilot-sharing scheme is better than the previous one, then there is a high probability that the exchanged scheme will be accepted. Conversely, if any AP cannot satisfy the synchronization requirements, then the pilot allocation scheme may hold the same with high probability.

⁵The swap operation is a two-sided version of the ‘‘exchange’’ considered in [28].

⁶Similar to the extremum of a multivariate function, it is impractical to obtain the globally optimal solution along the direction of one variable’s partial derivative while holding the other variables constant. Therefore, given the other pilot sharing scheme, the swap-matching operation can only maximize its own benefits while ignoring the other slave APs’ synchronization performance.

Algorithm 2 Pilot-Sharing based on Swap-Matching Algorithm

- 1: Initialize the first iteration number $n_1 = 1$, the maximum objective function $\text{Obj}_{\max} = 0$, $\text{Flag} = 1$, and the probability parameter T is 0.01;
 - 2: Initialize the maximum pilot overhead $\tau^{(n_1)} = \max\{|\mathcal{S}_1|, \dots, |\mathcal{S}_{K_C}|\}$, and the maximum number for reusing pilot sequences $N_{\max}^{(n_1)} = \left\lceil \frac{|\mathcal{S}_1 \cup \mathcal{S}_1 \dots \mathcal{S}_{K_C}|}{\tau^{(n_1)}} \right\rceil$;
 - 3: Use the Dastur algorithm to allocate the pilot sequences, denoted as $\mathcal{P}^{(n_1)} = \{\mathcal{P}_1, \dots, \mathcal{P}_{\tau^{(n_1)}}\}$;
 - 4: **while** ($\text{Flag} == 1$) **do**
 - 5: **if** ($\tau^{(n_1)} > L_S - 2K_C$) **then**
 - 6: $\text{Flag} = 0$;
 - 7: **else**
 - 8: Set the second iteration number n_2 to 1 and initialize the pilot sharing scheme as $\mathcal{P}^{(n_1, n_2)} = \mathcal{P}^{(n_1)}$;
 - 9: **while** $n_2 \leq N_2^{\max}$ **do**
 - 10: Update $n_2 = n_2 + 1$, randomly choose the proper slave APs and pilot sequence based on the two rules given in (50) and (52), and denote the switched pilot sharing scheme as \mathcal{P}^{sw} ;
 - 11: Calculate the objective functions for both two pilot sharing schemes, $\mathcal{P}^{(n_1, n_2-1)}$ and \mathcal{P}^{sw} , which are denoted as $\text{Obj}^{(n_1, n_2-1)}$ and Obj^{sw} , and update pilot sharing scheme $\mathcal{P}^{(n_1, n_2)}$ by executing the swap-matching operation with probability P_a ;
 - 12: **if** ($\text{Obj}^{\text{sw}} > \text{Obj}^{(n_1, n_2-1)}$) **then**
 - 13: Update the pilot sharing scheme $\mathcal{P} = \mathcal{P}^{\text{sw}}$ and $\text{Obj}_{\max} = \text{Obj}^{\text{sw}}$;
 - 14: **else**
 - 15: Update the pilot sharing scheme $\mathcal{P} = \text{Obj}^{(n_1, n_2-1)}$ and $\text{Obj}_{\max} = \text{Obj}^{(n_1, n_2-1)}$;
 - 16: **end if**
 - 17: **end while**
 - 18: Update $n_1 = n_1 + 1$, $\tau_p^{(n_1)} = \tau^{(n_1-1)} + 1$, $N_{\max}^{(n_1)} = \left\lceil \frac{|\mathcal{S}_1 \cup \mathcal{S}_1 \dots \mathcal{S}_{K_C}|}{\tau^{(n_1)}} \right\rceil$;
 - 19: Randomly select $(N_{\max}^{(n_1)} - 1)$ slave APs with low SINRs, replace their pilots with the $\tau^{(n_1)}$ -th pilot sequence, and denote the new pilot sharing scheme as $\mathcal{P}^{(n_1)}$;
 - 20: **end if**
 - 21: **end while**
-

In this way, we can keep tracking the optimal matching found in an iterative manner in a feasible region, i.e., $\tau \leq L_S - 2K_C$, even if the utility of the current matching is not locally optimal, which is detailed in Algorithm 2. Specifically, based on the coloring theory, in the n_1 -th iteration, the pilot overhead $\tau^{(n_1)}$ is initialized as the maximum number of slave APs in one cluster, and the maximum number for reusing one pilot sequence is determined by the number of slave APs and the pilot overhead, which is defined as

$$N_{\max}^{(n_1)} = \left\lceil \frac{|\mathcal{S}_1 \cup \mathcal{S}_1 \dots \mathcal{S}_{K_C}|}{\tau^{(n_1)}} \right\rceil, \quad (55)$$

where $\lceil \cdot \rceil$ means the ceiling function operation. If the total overhead is less than L_S , we begin to search the optimal solution. With the given pilot overhead $\tau^{(n_1)}$, the swap-matching operation is repeated until the number of iterations n_2 exceeds a specified number N_2^{\max} . Furthermore, after each swap-matching operation, the pilot sharing scheme with better performance is updated. In this way, the optimal pilot sharing scheme with pilot overhead $\tau^{(n_1)}$ can be found based on the synchronization requirements. Then, to keep tracking the optimal solution, a new pilot sequence will be introduced and allocated to the slave APs with low synchronization performance. Particularly, we update the number of iterations by $n_1 = n_1 + 1$, the pilot overhead by $\tau^{(n_1)} = \tau^{(n_1-1)} + 1$, and the number for reusing pilot sequence by $N_{\max}^{(n_1)} = \left\lceil \frac{|\mathcal{S}_1 \cup \mathcal{S}_1 \cdots \mathcal{S}_{K_C}|}{\tau^{(n_1)}} \right\rceil$. Then, we randomly select $(N_{\max}^{(n_1)} - 1)$ slave APs with low SINRs, denoting their indices as $\{i^{p_1}, \dots, i^{p_{N_{\max}^{(n_1)}-1}}\}$ and their pilot sequences as $\{p_1, \dots, p_{N_{\max}^{(n_1)}-1}\}$, $p_m \neq p_{m'}$ if $m \neq m'$. Furthermore, to follow the first rule, for given any two selected APs, i^{p_m} and $i^{p_{m'}}$, $\forall m, m' \in \{1, \dots, N_{\max}^{(n_1)} - 1\}$, $m \neq m'$, two APs are not in the common cluster, which is given by

$$i^{p_m} \cup i^{p_{m'}} \notin \mathcal{C}_k, \forall k \in \{1, \dots, K_C\}. \quad (56)$$

After that, the new pilot sequence is assigned to the selected slave APs, and the pilot sharing scheme in the n_1 -th iteration is updated, which is given by

$$\begin{aligned} \mathcal{P}_{p_m}^{(n_1)} &= \{\mathcal{P}_{p_m}^{(n_1-1)} \setminus i^{p_m}\}, \forall m \in \{1, \dots, N_{\max}^{(n_1)} - 1\}, \\ \mathcal{P}_{\tau^{(n_1)}}^{(n_1)} &= \{i^{p_1}, \dots, i^{p_{N_{\max}^{(n_1)}-1}}\}. \end{aligned} \quad (57)$$

Finally, based on the given clusters $\{\mathcal{C}_1, \dots, \mathcal{C}_{K_C}\}$, the optimal pilot sharing scheme is obtained by searching the feasible solutions.

To find the optimal solution to Problem (40), the above two algorithms are executed iteratively and the optimal solution is reserved, which is detailed in Algorithm 3.

D. Algorithm Analysis

In this subsection, the complexity of our proposed algorithm is analyzed. For the cluster classification algorithm, the average complexity is $O(L_C \times K \times I_c)$, where I_c is the number of iterations. For the pilot-sharing scheme, we need to search the optimal solution subject to the pilot overhead budget. Furthermore, for a given pilot overhead, the swap-matching operation needs to be executed N_2^{\max} times. The complexity of the pilot-sharing scheme is $O(N_2^{\max} \times I_\tau)$,

Algorithm 3 Resource Allocation for Problem (40)

- 1: Initialize iterative number $n = 0$ and the number of clusters $K_{\mathcal{C}}^n = 2$;
 - 2: Initialize the $\tau^n = 0$ and sum of CRBs as $\text{CRBs}^{(n)} = +\infty$;
 - 3: **while** ($\tau^n + 2K_{\mathcal{C}}^n \leq L_S$) **do**
 - 4: Update $n = n + 1$, execute Algorithm 1 with given $K_{\mathcal{C}}^n$, and obtain the clusters $\{\mathcal{C}_1, \dots, \mathcal{C}_{K_{\mathcal{C}}^n}\}$;
 - 5: Execute Algorithm 2 to obtain the pilot allocation scheme in the n -th iteration, denoted as $\{\mathcal{P}_1, \dots, \mathcal{P}_{\tau^n}\}$;
 - 6: Calculate the sum of CRBs, denoted as $\text{CRBs}^{(n)}$;
 - 7: Update $K_{\mathcal{C}}^{n+1} = K_{\mathcal{C}}^n + 1$;
 - 8: **if** ($\text{CRBs}^{(n)} < \text{CRBs}^{(n-1)}$) **then**
 - 9: Update cluster classification $\mathcal{C} = \{\mathcal{C}_1, \dots, \mathcal{C}_{K_{\mathcal{C}}^n}\}$ and pilot allocation $\mathcal{P} = \{\mathcal{P}_1, \dots, \mathcal{P}_{\tau^n}\}$;
 - 10: **end if**
 - 11: **end while**
-

where I_τ is the number of total iterations. Therefore, the complexity of our proposed algorithm lies in the number of both iterations of cluster classification and swap-matching operations.

V. SIMULATION RESULTS

In this section, the performance of our proposed pilot allocation strategy is numerically evaluated and discussed.

A. Simulation Parameters

There are K APs that are uniformly positioned constellation points in a smart factory of size 0.15×0.15 km². The large-scale fading factors are based on the Hata-COST231 propagation model of [2], where the height of each AP is 15 m. Specifically, the three-slope path loss (dB) can be expressed as

$$\text{PL}_{m,k} = \begin{cases} L_{\text{loss}} + 35\log_{10}(d_{m,k}), & d_{m,k} > d_1 \\ L_{\text{loss}} + 15\log_{10}(d_1) + 20\log_{10}(d_{m,k}), & d_0 < d_{m,k} \leq d_1, \\ L_{\text{loss}} + 15\log_{10}(d_1) + 20\log_{10}(d_0), & d_{m,k} \leq d_0 \end{cases} \quad (58)$$

where $d_{m,k}$ is the distance between the m -th AP and the k -th AP, L_{loss} is a constant of 140.7 (dB), while d_0 and d_1 are 0.01 km and 0.05 km, respectively. Furthermore, each AP's transmission power is 1 W.

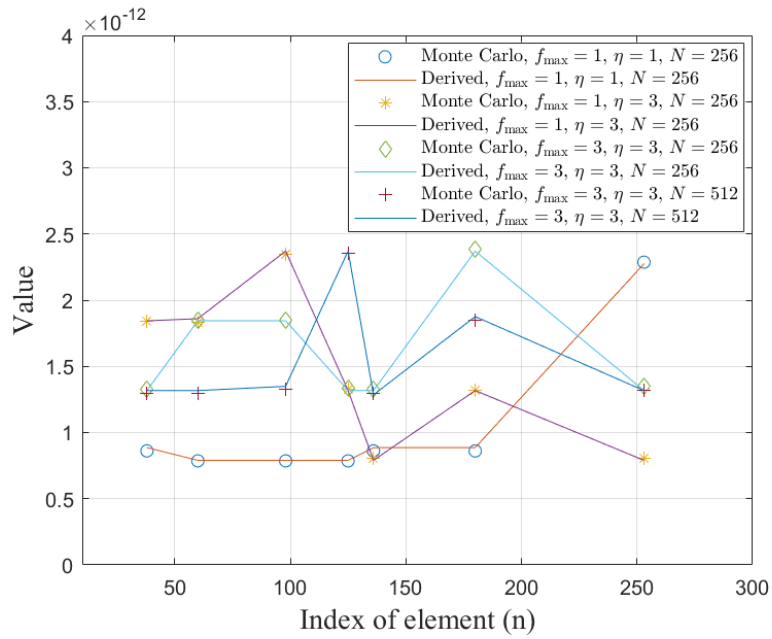


Fig. 4: $[D_{i,j_k}]_{n,n}$ based on Monte-Carlo simulation and derived result.

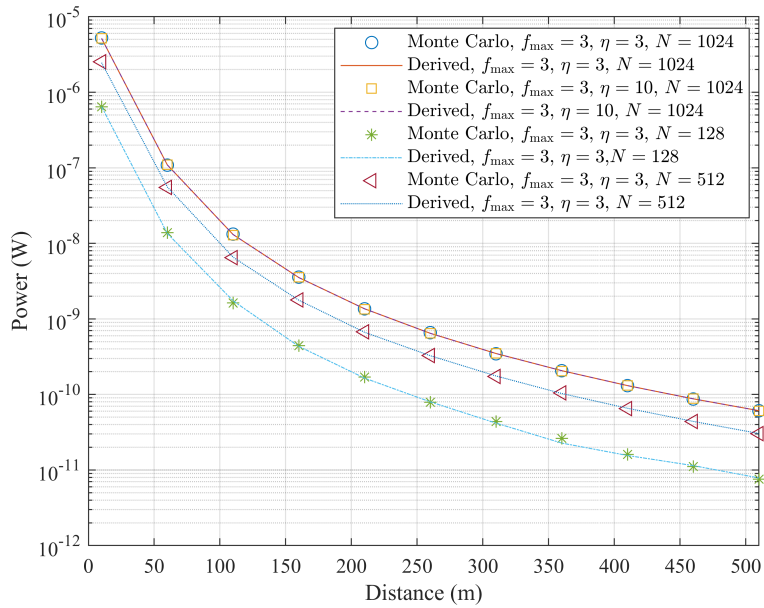


Fig. 5: Power of Pilot Contamination based on Monte-Carlo simulation and derived result.

B. Derivation and Monte-Carlo Simulations

To check whether our derivations can provide a more convenient expression for the pilot sharing scheme, we first check the $[n, n]$ -th element of \mathbf{D}_{i,j_k} based on Monte-Carlo simulations and derived result. Fig. 4 depicts the randomly chosen elements of \mathbf{D}_{i,j_k} with different CFOs, TOs, and pilot lengths. Monte-Carlo simulation is consistent with our derived closed-form expression, which demonstrates the accuracy of our derivations.

To investigate the relationship between the distance-based large-scale fading factor and the power of pilot contamination, we depict the power of derived pilot contamination and that based on Monte-Carlo simulations. Fig. 5 shows the power with a pilot sequence \mathbf{s} formed by various lengths N in the binary phase shift keying (BPSK) constellation. Obviously, our derived results are consistent with Monte-Carlo simulations, demonstrating that our derived result can provide an explicit expression for the latter pilot-sharing scheme. Furthermore, we observe that the power of pilot contamination increases with the pilot length N . This is due to the fact that the power is equal to the trace of the matrix, which increases with the pilot length N . More importantly, it is worth noting that the power of pilot contamination has no significant relationship between the CFO and TO but significantly decreases with the increased distance, which demonstrates the effectiveness of our derivations.

C. Cramer-Rao Bound and ML Estimation

To verify our derivations, we first check the theoretical lower bound, i.e., CRB, and the MSE based on ML estimation. Fig. 6 depicts the synchronization performance with various SNRs. Furthermore, to obtain the inverse matrix, the large-scale fading factor of each path is normalized by dividing the maximum large-scale fading factor from the slave AP to master AP. Apparently, the CRBs and MSEs of ML estimation decrease with the increased SNR, especially for the results without pilot contamination. This phenomenon arises due to the diminished interference between the desired signal and noise when the SNR is high, resulting in better synchronization performance. However, owing to the pilot sharing, the lower bound based on the pilot contamination no longer linearly decreases with SNR, but instead experiences a flat trend. This is due to the fact that as the noise power decreases, the main factor affecting the estimation performance is no longer the noise, but the pilot contamination.

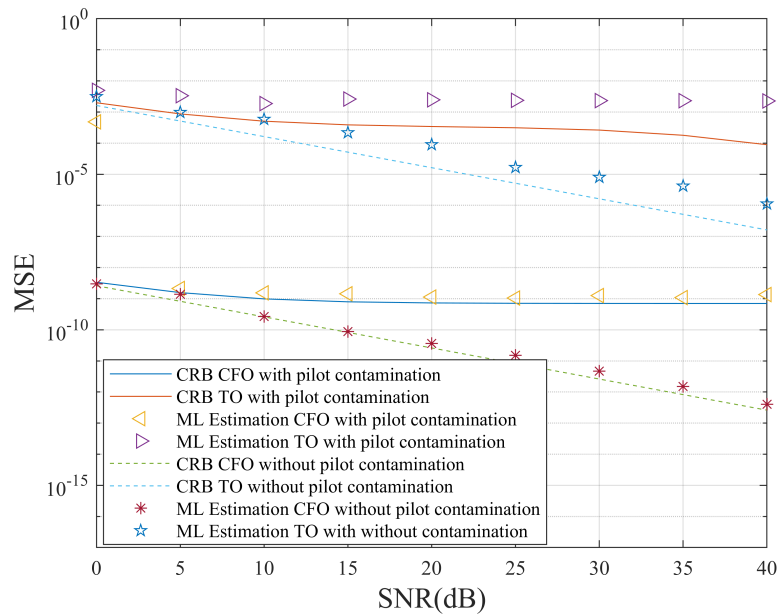


Fig. 6: CRB and ML estimation versus SNRs with path delay $[0, 0.7049T_s, 2.1230T_s, 2.7063T_s]$, path gain $[1, 0.8443, 0.4119, 0.3223]$, and large-scale fading factor 5.16×10^{-10} .

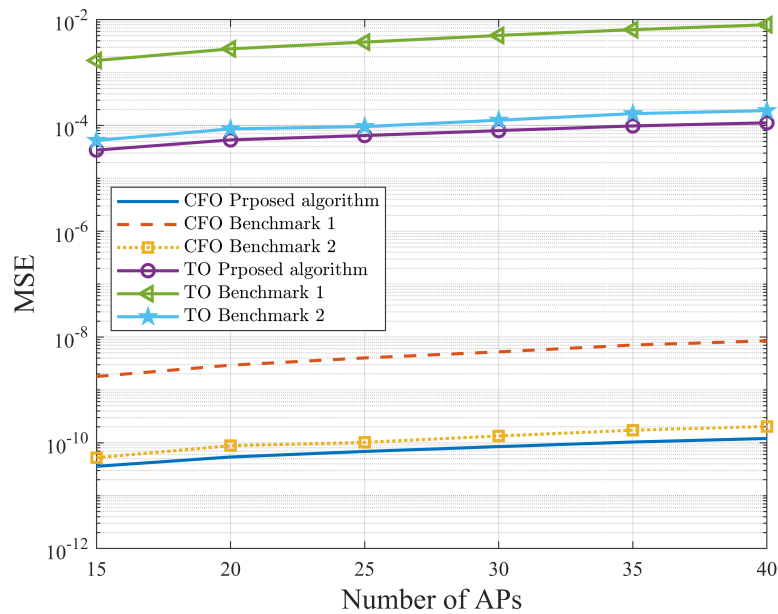


Fig. 7: Sum of CRBs versus the number of APs with $N = 256$, $\eta = 3$, $f_{\max} = 3$, $\text{SINR}^{\min} = 15$ dB.

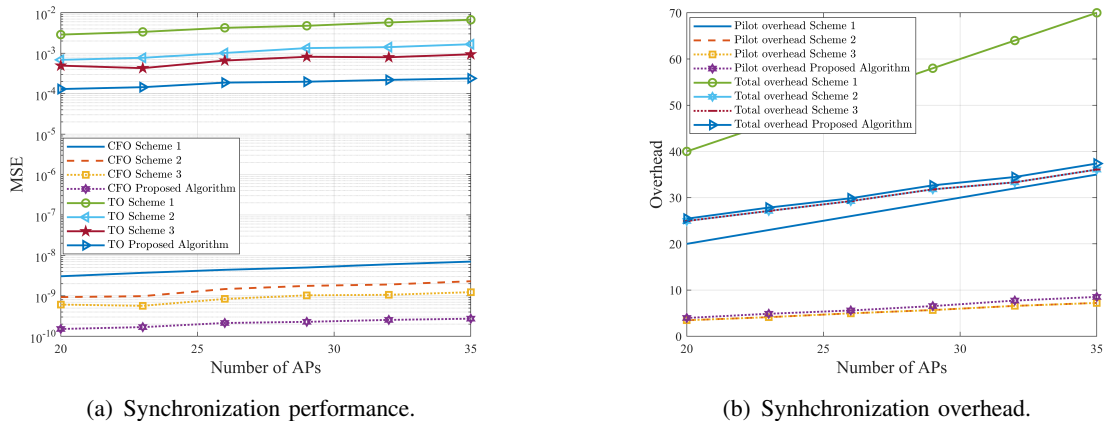


Fig. 8: Sum of CRBs versus the number of APs with $N = 256$, $\eta = 3$, $f_{\max} = 3$, $\text{SINR}^{\min} = 15$ dB, $L_S = [25, 28, 31, 34, 37, 40]$.

D. Performance of the Proposed Algorithm

To investigate the impact of clustering on the synchronization performance, we assume that the K APs are randomly distributed in this area and all slave APs are allocated to a unique pilot sequence. Furthermore, to illustrate the performance of our adaptive cluster classification, we also compare our approach with the following two benchmarks:

Benchmark 1: All slave APs transmit pilot sequences directly to the CPU, whose 2-dimensional location is $[0,0]$.

Benchmark 2: The clusters are classified by the K-means algorithm while the master APs are randomly chosen in each cluster.

By averaging over 100 simulation results where the path delays and path gain coefficients are randomly generated, Fig. 7 illustrates the sum of CRBs of all slave APs. Obviously, the synchronization performance slightly increases with the number of APs. Furthermore, it is worth noting that our approach is superior to all benchmarks. This is due to the fact that the cluster classification could shorten the distance between master and slave APs, thereby improving the path gain and enhancing the estimation performance. Additionally, in each cluster, the synchronization performance is further improved by reducing the distance between master APs and slave APs.

To further investigate the performance of our pilot sharing algorithm, we also compare our algorithm with the following pilot allocation schemes.

Scheme 1: All slave APs transmit orthogonal pilot sequences directly to the CPU, whose

2-dimensional location is $[0,0]$.

Scheme 2: The clusters are classified by the K-means algorithm while the master APs are randomly chosen in each cluster, and the pilot sharing scheme is obtained by using the Dastur algorithm.

Scheme 3: The clusters are classified by using our adaptive cluster algorithm, and the pilot sharing scheme is obtained by using the Dastur algorithm.

Fig. 8(a) illustrates the averaged sum of CRBs under the case of various numbers of APs, while Fig. 8(b) shows the averaging overhead of each scheme. As can be seen from Fig. 8(a), the synchronization performance slightly increases with the number of APs. For Scheme 1, owing to the lower path gain, the estimation errors are unable to meet the synchronization requirements. Even though sharing pilots causes pilot contamination between APs, the distance among APs that use the common pilot sequence is maximized to meet the synchronization requirements. Furthermore, benefiting from our proposed algorithm, the estimation errors are comparatively stable in the demand range.

VI. CONCLUSIONS

To investigate the impact of synchronous pilot sharing on the estimation performance, we derived the CRB while considering the pilot contamination, and the results revealed that the estimation error is strongly related to the power of pilot contamination, especially for the high SNR regime. Furthermore, a maximum likelihood algorithm was presented to estimate the CFO and TO among the pairing APs. Then, to minimize the sum of CRBs, a synchronization strategy based on the pilot-sharing scheme was devised by jointly optimizing the cluster classification, synchronization overhead, and pilot-sharing scheme. This NP-hard problem was simplified into two sub-problems, including cluster classification and the pilot sharing scheme. Specifically, the clusters were classified by combining the K-means algorithm with the minimum distance sum criterion, while the pilot sharing scheme was obtained using swap-matching operations. Simulation results validated the accuracy of our derivations and demonstrated the effectiveness of the proposed scheme over other pilot-pair algorithms.

APPENDIX A
PROOF OF (8)

The $[k', l]$ -th element of $\mathbf{S}_p \mathbf{U}(\Delta\tau_{i,j_k})$ is given by

$$\begin{aligned}
[\mathbf{S}_p \mathbf{U}(\Delta\tau_{i,j_k})]_{k',l} &= \sum_{n=1}^{M-N+1} [\mathbf{S}_p]_{k',n} [\mathbf{U}(\Delta\tau_{i,j_k})]_{n,l} \\
&= \sum_{n=1}^{M-N+1} [\mathbf{S}_p]_{k',n} \nabla\left(n - 1 - \frac{\Delta\tau_{i,j_k} + \varsigma_{i,j_k}^l}{T_s}\right) \\
&= \sum_{n=1}^{M-N+1} s_p^{k'-n} \nabla\left(n - 1 - \frac{\Delta\tau_{i,j_k} + \varsigma_{i,j_k}^l}{T_s}\right),
\end{aligned} \tag{59}$$

where $s_p^{k'-n}$ is 0 when $k' - n < 0$ and $k' - n > N - 1$.

Based on the definition of $\nabla(t)$, we have

$$\nabla(t) = \begin{cases} t, & 0 < t \leq 1 \\ 2 - t, & 1 < t \leq 2 \\ 0, & \text{otherwise.} \end{cases} \tag{60}$$

By substituting (60) into (59), we have

$$[\mathbf{S}_p \mathbf{U}(\Delta\tau_{i,j_k})]_{k',l} = s_p^{k'-x_1} \nabla\left(x_1 - 1 - \frac{\Delta\tau_{i,j_k} + \varsigma_{i,j_k}^l}{T_s}\right) + s_p^{k'-x_1-1} \nabla\left(x_1 - \frac{\Delta\tau_{i,j_k} + \varsigma_{i,j_k}^l}{T_s}\right), \tag{61}$$

where x_1 is $\left\lceil 1 + \frac{\Delta\tau_{i,j_k} + \varsigma_{i,j_k}^l}{T_s} \right\rceil$.

Then, letting $k' - x_1 = n$, $k' \in \{1, \dots, M\}$, we have

$$\begin{aligned}
[\mathbf{S}_p \mathbf{U}(\Delta\tau_{i,j_k})]_{k',l} &= s_p^n \nabla\left(k' - 1 - n - \frac{\Delta\tau_{i,j_k} + \varsigma_{i,j_k}^l}{T_s}\right) + s_p^{n-1} \nabla\left(k' - n - \frac{\Delta\tau_{i,j_k} + \varsigma_{i,j_k}^l}{T_s}\right) \\
&= \sum_{n=0}^{N-1} s_p^n \nabla\left(k' - 1 - n - \frac{\Delta\tau_{i,j_k} + \varsigma_{i,j_k}^l}{T_s}\right).
\end{aligned} \tag{62}$$

Finally, we substitute $m = k' - 1$ into (62) and complete the proof of (8) by combining the results of $\mathbf{F}(\Delta f_{i,j_k})$ and \mathbf{h}_{i,j_k} .

REFERENCES

- [1] G. Interdonato, E. Björnson, H. Quoc Ngo, P. Frenger, and E. G. Larsson, "Ubiquitous cell-free massive MIMO communications," *EURASIP J. Wireless Commun. and Netw.*, vol. 2019, no. 1, pp. 1–13, Dec. 2019.
- [2] H. Q. Ngo, A. Ashikhmin, H. Yang, E. G. Larsson, and T. L. Marzetta, "Cell-free massive MIMO versus small cells," *IEEE Trans. Wireless Commun.*, vol. 16, no. 3, pp. 1834–1850, 2017.

- [3] Q. Peng, H. Ren, C. Pan, N. Liu, and M. ElKashlan, "Resource allocation for uplink cell-free massive MIMO enabled URLLC in a smart factory," *IEEE Trans. Commun.*, vol. 71, no. 1, pp. 553–568, 2022.
- [4] C.-X. Wang, X. You, X. Gao, X. Zhu, Z. Li, C. Zhang, H. Wang, Y. Huang, Y. Chen, H. Haas *et al.*, "On the road to 6G: Visions, requirements, key technologies and testbeds," *IEEE Commun. Sur. Tuts.*, vol. 25, no. 2, pp. 905–974, 2nd Quar. 2023.
- [5] H. Q. Ngo, L.-N. Tran, T. Q. Duong, M. Matthaiou, and E. G. Larsson, "On the total energy efficiency of cell-free massive MIMO," *IEEE Trans. Green Commun. Netw.*, vol. 2, no. 1, pp. 25–39, Mar. 2018.
- [6] E. Björnson and L. Sanguinetti, "Making cell-free massive MIMO competitive with MMSE processing and centralized implementation," *IEEE Trans. Wireless Commun.*, vol. 19, no. 1, pp. 77–90, 2019.
- [7] —, "Scalable cell-free massive MIMO systems," *IEEE Trans. Commun.*, vol. 68, no. 7, pp. 4247–4261, Jul. 2020.
- [8] H. Yan and I.-T. Lu, "Asynchronous reception effects on distributed massive MIMO-OFDM system," *IEEE Trans. Commun.*, vol. 67, no. 7, pp. 4782–4794, 2019.
- [9] J. Li, M. Liu, P. Zhu, D. Wang, and X. You, "Impacts of asynchronous reception on cell-free distributed massive MIMO systems," *IEEE Trans. Veh. Technol.*, vol. 70, no. 10, pp. 11 106–11 110, 2021.
- [10] H. Sallouha, A. Chiumento, S. Rajendran, and S. Pollin, "Localization in ultra narrow band IoT networks: Design guidelines and tradeoffs," *IEEE Internet Things J.*, vol. 6, no. 6, pp. 9375–9385, 2019.
- [11] H. V. Balan, R. Rogalin, A. Michaloliakos, K. Psounis, and G. Caire, "Airsync: Enabling distributed multiuser MIMO with full spatial multiplexing," *IEEE/ACM Trans. Netw.*, vol. 21, no. 6, pp. 1681–1695, 2013.
- [12] O. Abari, H. Rahul, D. Katabi, and M. Pant, "Airshare: Distributed coherent transmission made seamless," in *Proc. IEEE Conf. Comput. Commun. (INFOCOM)*. IEEE, 2015, pp. 1742–1750.
- [13] K. Alemdar, D. Varshney, S. Mohanti, U. Muncuk, and K. Chowdhury, "Rfclock: Timing, phase and frequency synchronization for distributed wireless networks," in *Proc. Int. Conf. Mobile Computing and Netw.*, 2021, pp. 15–27.
- [14] M. Rashid and J. A. Nanzer, "Frequency and phase synchronization in distributed antenna arrays based on consensus averaging and kalman filtering," *IEEE Trans. Wireless Commun.*, vol. 22, no. 4, pp. 2789–2803, 2022.
- [15] K. Matsuura, K. Shin, D. Kobuchi, Y. Narusue, and H. Morikawa, "Synchronization strategy for distributed wireless power transfer with periodic frequency and phase synchronization," *IEEE Commun. Lett.*, vol. 27, no. 1, pp. 391–395, 2022.
- [16] S. R. Mghabghab, A. Schlegel, and J. A. Nanzer, "Adaptive distributed transceiver synchronization over a 90 m microwave wireless link," *IEEE Trans. Antenn. Propag.*, vol. 70, no. 5, pp. 3688–3699, 2022.
- [17] R. Rogalin, O. Y. Bursalioğlu, H. Papadopoulos, G. Caire, A. F. Molisch, A. Michaloliakos, V. Balan, and K. Psounis, "Scalable synchronization and reciprocity calibration for distributed multiuser MIMO," *IEEE Trans. Wireless Commun.*, vol. 13, no. 4, pp. 1815–1831, 2014.
- [18] Y. Feng, W. Zhang, Y. Ge, and H. Lin, "Frequency synchronization in distributed antenna systems: Pairing-based multi-CFO estimation, theoretical analysis, and optimal pairing scheme," *IEEE Trans. Commun.*, vol. 67, no. 4, pp. 2924–2938, 2018.
- [19] U. K. Ganesan, R. Sarvendranath, and E. G. Larsson, "Beamsync: Over-the-air synchronization for distributed massive MIMO systems," *IEEE Trans. Wireless Commun.*, 2023.
- [20] M. Attarifar, A. Abbasfar, and A. Lozano, "Random vs structured pilot assignment in cell-free massive MIMO wireless networks," in *Proc. IEEE Int. Conf. Commun. Workshops (ICCW)*, Jul. 2018, pp. 1–6.
- [21] H. Liu, J. Zhang, X. Zhang, A. Kurniawan, T. Juhana, and B. Ai, "Tabu-search-based pilot assignment for cell-free massive MIMO systems," *IEEE Trans. Veh. Technol.*, vol. 69, no. 2, pp. 2286–2290, Feb. 2020.
- [22] S. Buzzi, C. D'Andrea, M. Fresia, Y.-P. Zhang, and S. Feng, "Pilot assignment in cell-free massive MIMO based on the hungarian algorithm," *IEEE Wireless Commun. Lett.*, vol. 10, no. 1, pp. 34–37, Jan. 2021.

- [23] H. Liu, J. Zhang, S. Jin, and B. Ai, "Graph coloring based pilot assignment for cell-free massive MIMO systems," *IEEE Trans. Veh. Technol.*, vol. 69, no. 8, pp. 9180–9184, Aug. 2020.
- [24] W. Zeng, Y. He, B. Li, and S. Wang, "Pilot assignment for cell free massive MIMO systems using a weighted graphic framework," *IEEE Trans. Veh. Technol.*, vol. 70, no. 6, pp. 6190–6194, Jun. 2021.
- [25] Q. Peng, H. Ren, M. Dong, M. ElKashlan, K.-K. Wong, and L. Hanzo, "Resource allocation for cell-free massive MIMO-aided URLLC systems relying on pilot sharing," *IEEE J. Sel. Areas Commun.*, vol. 41, no. 7, pp. 2193–2207, Jul. 2023.
- [26] T. Kanungo, D. M. Mount, N. S. Netanyahu, C. D. Piatko, R. Silverman, and A. Y. Wu, "An efficient k-means clustering algorithm: Analysis and implementation," *IEEE Trans. Pattern Anal. Machine Intelligence*, vol. 24, no. 7, pp. 881–892, 2002.
- [27] C. Pan, H. Mehrpouyan, Y. Liu, M. ElKashlan, and N. Arumugam, "Joint pilot allocation and robust transmission design for ultra-dense user-centric TDD C-RAN with imperfect CSI," *IEEE Trans. Wireless Commun.*, vol. 17, no. 3, pp. 2038–2053, 2018.
- [28] E. Bodine-Baron, C. Lee, A. Chong, B. Hassibi, and A. Wierman, "Peer effects and stability in matching markets," in *International Symposium on Algorithmic Game Theory*. Springer, 2011, pp. 117–129.